ARR Nov. 1941

NATIONAL ADVISORY COMMITTEE FOR AERONAUTICS

WARTIME REPORT

ORIGINALLY ISSUED
November 1941 as
Advance Restricted Report

WIND-TUNNEL TESTS OF EIGHT-BLADE SINGLE- AND DUAL-ROTATING PROPELLERS IN THE TRACTOR POSITION

By David Biermann and W. H. Gray

Langley Memorial Aeronautical Laboratory
Langley Field, Va.

NACA

WASHINGTON

WIND TUNNEL TESTS OF EIGHT-BLADE SINGLE- AND DUAL-ROTATING PROPELLERS IN THE TRACTOR POSITION

By David Biermann and W. H. Gray

SUMMARY

Tests of 10-foot diameter, eight-blade single- and dual-rotating propellers were conducted in the 20-foot propeller-research tunnel as a continuation of a previous investigation of four- and six-blade propellers. The propellers were mounted at the front end of a streamline body in spinners that covered the hubs and part of the shanks. The effect of a symmetrical wing mounted in the slipstream was investigated. Blade-angle settings ranged from 20° to 65°.

The results indicate that dual rotation resulted in gains of 1 to 8 percent in efficiency over single rotation for eight-blade propellers, but the presence of a wing reduced the gain by about one-half. Also indicated was a greater power absorption due to dual rotation over the entire flight range, and higher efficiency or thrust for the range of take-off and climb.

INTRODUCTION

A report previously released (reference 1) presented results of tests of four- and six-blade dual- and single-rotating tractor propellers. The present report describes the results of a subsequent investigation of eight-blade single- and dual-rotating propellers mounted in the tractor position on the same set-up as that previously used. The effect of a symmetrical wing mounted in the slipstream was included in the investigation as before.

APPARATUS AND METHODS

Inasmuch as the present investigation is a continuation of one previously made in the propeller-research tunnel (see reference 1), a detailed description of the apparatus and methods will not be repeated here. A short description is included, however, in order to make this report fairly complete within itself.

Propellers.- Both the eight-blade single- and dual-rotating propellers were mounted in four-way hubs spaced $9\frac{15}{16}$ inches apart (see figs. 1 and 2), thereby providing identical blade shank and spinner conditions. Preliminary tests were made to determine the optimum angular displacement between the front and rear propeller blades for the single-rotation tests; the blades of the front propeller were set to lead the blades of the rear propeller by 75°, $52\frac{1}{2}$°, and 30°. Although the results indicated little difference between these three spacings, the $52\frac{1}{2}$° spacing was considered the best. Equal spacing of 45° was not possible owing to a limitation imposed by the shaft spline.

The blades used for the present investigation were the same as previously tested, namely, Hamilton Standard 3155-6 and 3156-6, right-hand and left-hand, respectively. Blade-form curves are given in figure 3. Clark Y sections are incorporated throughout.

Test conditions.- Because of the limiting tunnel speed (approximately 110 mph) and the limiting power of the drive motors (two 25 hp electric motors), the Reynolds number and the tip speed were considerably lower than those experienced in flight. The maximum propeller speed, which was 550 rpm, was obtainable only for the low blade angles and the low V/nD range of the tests. The tip speed, consequently, was below 300 feet per second, and thus the effect of compressibility could not be measured. The Reynolds number of the 0.75R section was only of the order of one million. The effect of Reynolds number was not critical within the range of the tests as the effect of changes between one-half million and one million could not be measured.

The left-hand (front) propeller was set at even values of blade setting for the dual-rotation tests. The right-hand (rear) propeller was set to absorb the same power as the left-hand propeller for only the peak efficiency condition. A plot of the angular difference between the right-hand and the left-hand propeller-blade settings is given in figure 4. The speed of the right- and the left-hand propellers was maintained equal throughout the tests. The test procedure was the same as that used for previous investigations in this tunnel.

RESULTS AND DISCUSSION

The measured values have been reduced to the usual coefficients of thrust, power, and propulsive efficiency,

$$C_T = \frac{\text{effective thrust}}{\rho\, n^2\, D^4}$$

$$C_P = \frac{\text{engine power}}{\rho\, n^3\, D^5}$$

$$C_s = \sqrt[5]{\frac{\rho V^5}{P n^2}}$$

where the effective thrust is the measured thrust of the propeller-body combination plus the drag of the body measured separately.

D propeller diameter, feet

n propeller rotational speed, revolutions per second

ρ mass density of the air, slugs per cubic foot

These coefficients were plotted against V/nD. The results are given in the following figures:

Figures

5 - 7 Characteristic curves for eight-blade propeller, single rotation without wing

8 - 11 Characteristic curves for eight-blade propeller, dual rotation without wing

12 - 15 Characteristic curves for eight-blade propeller, single rotation with wing

The general characteristics of eight-blade single- and dual-rotating propellers, shown in figures 5 to 20, indicate that the principal effect of the increased solidity over that for the four- and six-blade propellers reported in reference 1 was increased total power absorption with little loss in blade efficiency.

Effect of dual rotation on total power absorbed.- Of particular interest is the fact that the dual-rotating propellers absorbed appreciably more power than did the single-rotating one, as may be noted in figures 16 to 19, wherein the characteristic curves obtained for several angle settings for single rotation are superimposed on those for dual rotation. This increased power absorption may be accounted for by the fact that the front propeller introduced a rotational component to the slipstream, which increased the resultant velocity over the rear propeller blades. This rotational component is greatest when the blade elements meet the relative air with the greatest angles of attack, so the effect was more noticeable at low V/nD values than for the high V/nD values. This increased power-absorption characteristic of dual-rotating propellers is one explanation for their resulting superior take-off qualities, owing to the fact that for this condition the pitch is reduced to a lower value than for single-rotating propellers.

A comparison is made in figure 21 wherein the power absorbed at peak efficiency per blade, relative to that for the blades of a three-blade propeller, is presented for both single- and dual-rotating propellers. This plot indicates that the effectiveness of each blade of the dual propeller in absorbing power was substantially more than that for a single-rotating propeller; the individual blades of an eight-blade dual propeller absorbed approximately 87 percent as much power as each blade of a three-blade single propeller, as compared to only 80 percent for an eight-blade single propeller.

Effect of dual rotation on power absorbed by rear propeller.- The dual-rotation tests were conducted with the rear propeller set at a slightly lower angle than the front one in order to equalize the power for the peak efficiency condition. The rear propeller absorbed more power than the front one at lower V/nD values than those for peak efficiency. A few tests were made to determine the blade settings of the rear propeller necessary to produce equal power absorption; the results of these tests are shown in figures 22 and 23. Whether there is any aerodynamic advantage in equalizing the power of the two propellers for the take-off and climbing conditions of flight cannot be determined from these tests because direct efficiency comparisons cannot be made on a basis of equal power absorption.

Envelope efficiency comparisons.- The same general improvement in efficiency due to dual rotation may be noted in figure 24 for the eight-blade propellers as for the earlier tests of four- and six-blade propellers. The gain in efficiency due to dual rotation, without the wing, ranged from about 1 to 8 percent, depending upon the blade angle or V/nD, which is somewhat greater than that measured in the four- and six-blade tests. The gains were somewhat less with the wing in place, owing to its effect in reducing the rotational losses for the single-rotating propeller. The wing appeared to have a slight beneficial effect on the dual propellers, as may be noted in figure 25. This same effect, which is not easily accounted for, was also indicated in the earlier tests of the four- and six-blade propellers.

In figures 26 and 27 are shown the envelope efficiency curves for the present eight-blade propellers and curves for four- and six-blade propellers, obtained from reference 1 for comparison. The general effect of increasing the solidity for single rotation without the wing, shown in figure 26(a), was to reduce the efficiency a few percent over the V/nD range. The presence of the wing resulted in raising the efficiency of all these single-rotating propellers, particularly those of highest solidity. (See fig. 26(b).) The loss in efficiency resulting from increasing the solidity was generally less for dual rotation than for single rotation, as may be noted from figures 26 and 27, particularly for the condition without wing.

It should be pointed out that envelope efficiency comparisons for propellers of different solidity are more of an academic interest than of practical value because of the fact that the power absorption is different for different solidities. Such comparisons provide a measure of blade efficiency, or the effect of blade interference. From engineering design considerations the comparisons should be made on the basis of constant power. Such comparisons of solidity are provided in reference 2.

The effects of dual rotation on the peak efficiency for four-, six-, and eight-blade propellers are summarized in figures 28 and 29. Although the results are not of sufficient accuracy to define differences in efficiency less than 1 percent, they show, in general, that the gain arising from dual-rotating propellers increases with the blade angle or V/nD, and also with propeller solidity. The gains were somewhat greater for the condition without the wing than with the wing (7 percent as compared with $4\frac{1}{2}$ percent, for V/nD of 5.0, eight-blade propeller.)

Efficiency and thrust comparisons at constant power.- Inasmuch as the dual-rotating propellers absorbed somewhat more power at the same blade setting than the single-rotating propellers, the effect of dual rotation on efficiency should be based on equal power absorption. Comparisons are made in figures 30 to 32 for C_P values of 0.2, 0.4, and 0.6. Substantial gains in efficiency may be noted for the entire operating range, particularly for the take-off condition of propellers operating at high values of C_P. These efficiency gains are translated into thrust gains in figure 33. Take-off thrust gains up to 20 percent are indicated for dual propellers operating at a power coefficient of 0.6; somewhat less for lower power coefficients. This increased thrust may be accounted for partly by the fact that dual-rotating propellers absorbed more power than single-rotating ones as mentioned before and, consequently, the blade-angle settings for the dual propellers were computed to be somewhat lower than for single-rotating propellers; particularly for the take-off and climb conditions. This lower blade-angle setting results in greater thrust for a given power output, owing to the higher lift-drag ratios of the elements. Also with dual propellers the losses due to slipstream rotation are greatly reduced and perhaps eliminated, which accounts for a large percentage of the gain in efficiency.

CONCLUSIONS

The general effects of dual rotation on propeller characteristics found in previous tests of four- and six-blade propellers were similar, but were more pronounced in the present investigation of eight-blade propellers. These effects are listed more specifically in the following conclusions relating to the present investigation.

1. The peak efficiency of an eight-blade dual-rotating propeller was found to be from 1 to 8 percent higher than that for a corresponding single-rotating propeller. The gain in efficiency depended upon the blade-angle setting, the higher the setting the greater the gain, up to a limiting test blade-angle of 65°.

2. The presence of a wing in the slipstream improved the efficiency of the single-rotating propeller about half as much as was obtained by means of dual rotation.

3. An eight-blade dual-rotating propeller was found to absorb substantially more power at peak efficiency than an eight-blade single-rotating propeller; the effect was even more pronounced at take-off and climbing conditions.

4. An eight-blade dual-rotating propeller was found to be substantially more efficient for the take-off condition of flight than an eight-blade single-rotating propeller, particularly for conditions of operation at high power coefficients.

5. The blade efficiency of eight-blade single- and dual-rotating propellers was only slightly less than for corresponding four- and six-blade propellers previously tested.

6. The power absorbed per blade by eight-blade dual-rotation and eight-blade single-rotation propellers, as compared to a three-blade propeller, was about 87 and 80 percent, respectively, at peak efficiency.

Langley Memorial Aeronautical Laboratory,
National Advisory Committee for Aeronautics,
Langley Field, Va.

REFERENCES

1. Biermann, David, and Hartman, Edwin P.: Wind-Tunnel Tests of Four- and Six-Blade, Single- and Dual-Rotating Tractor Propellers. NACA Rep. No. 747, 1942.

2. Biermann, David, and Conway, Robert N.: The Selection of Propellers for High Thrust at Low Airspeed. NACA ARR, Oct. 1941.

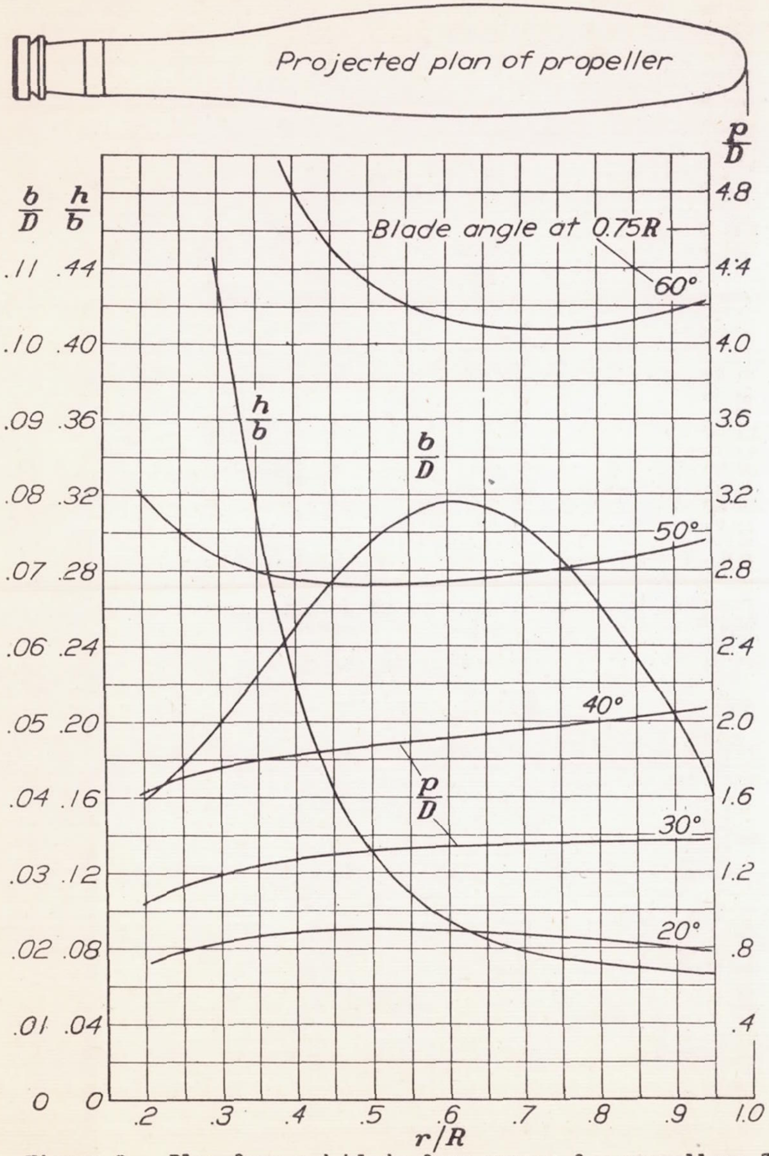

Figure 3.- Plan-form and blade-form curves for propellers 3155-6 and 3156-6. D, diameter; R, radius to the tip; r, station radius; b, section chord; h, section thickness; p, geometric pitch.

Note: Front and rear nacelle lines are identical.

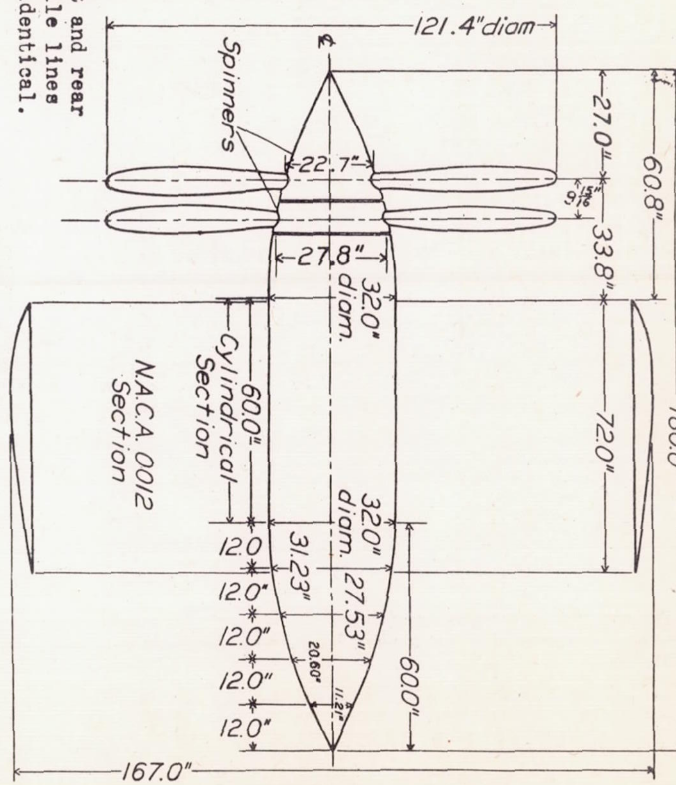

Figure 1.- Plan view showing dimensional details of wing and nacelle.

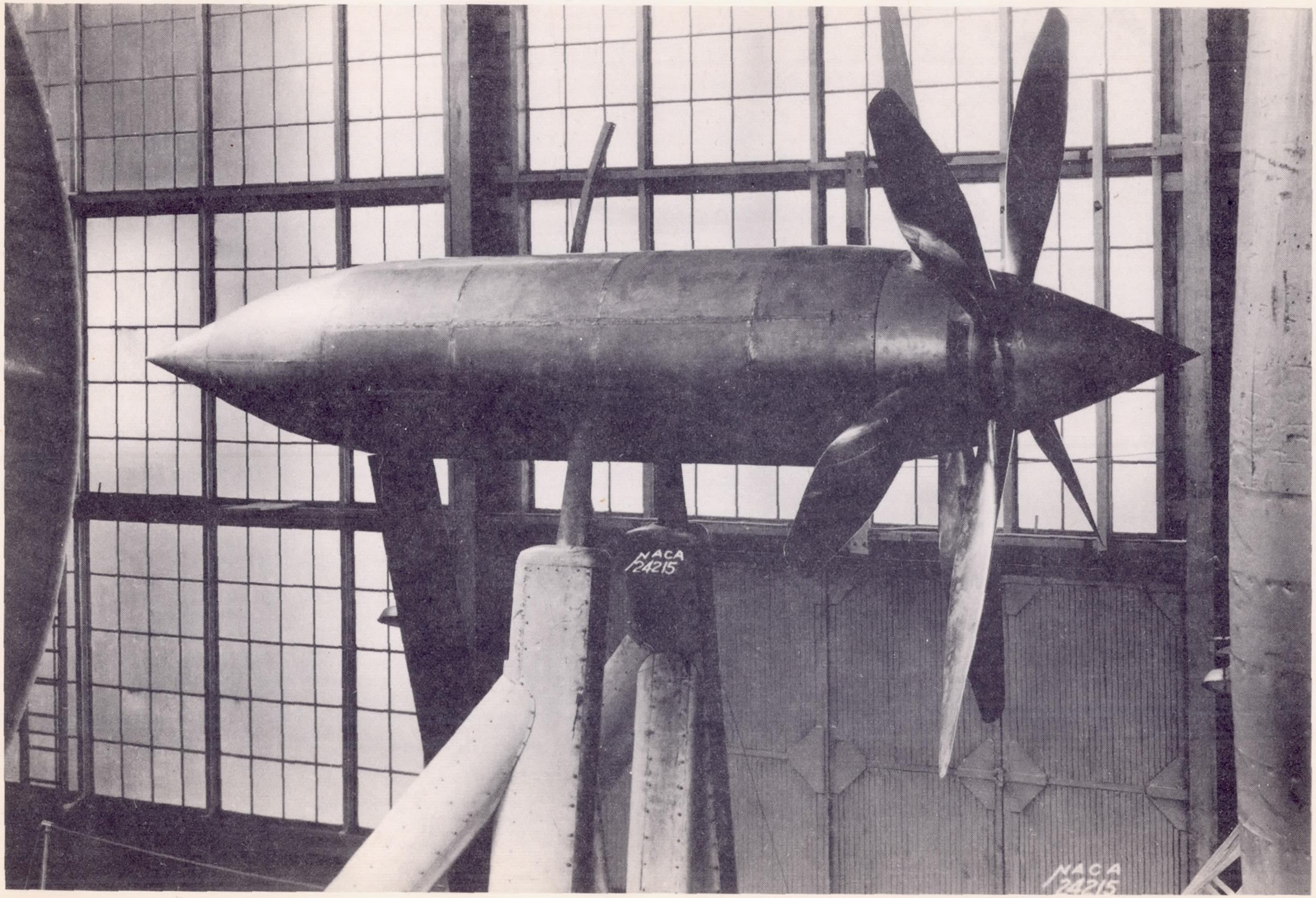

Figure 2.- Test set-up. Eight-blade dual-rotation propeller installed.

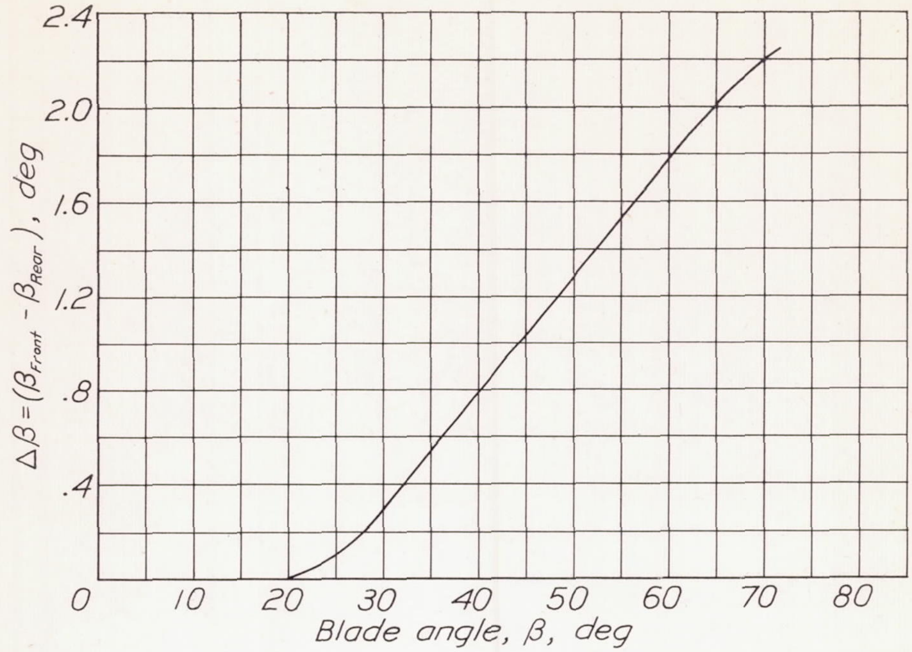

Figure 4.- Difference in blade angle for equal torque at peak efficiency for, eight blades, dual rotation.

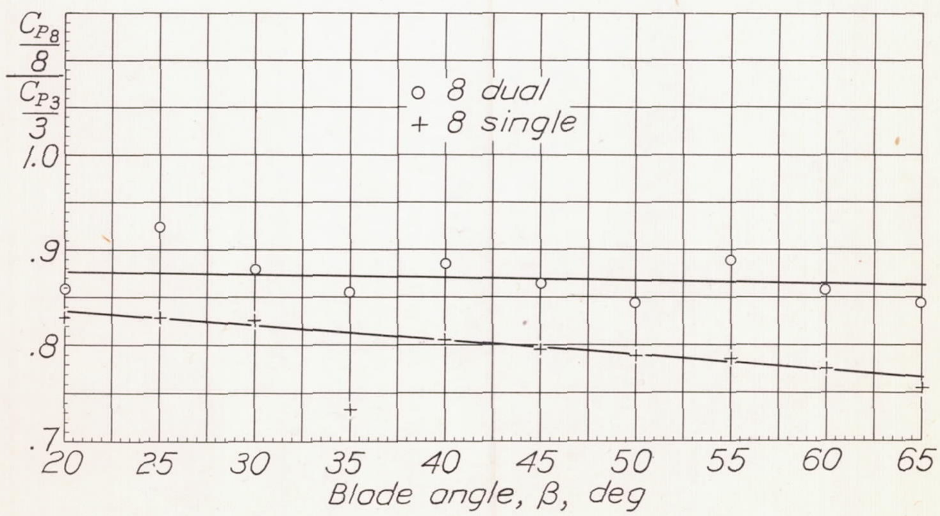

Figure 21.- Ratio of power absorbed at peak efficiency per blade for eight-and three-blade propellers. With wing.

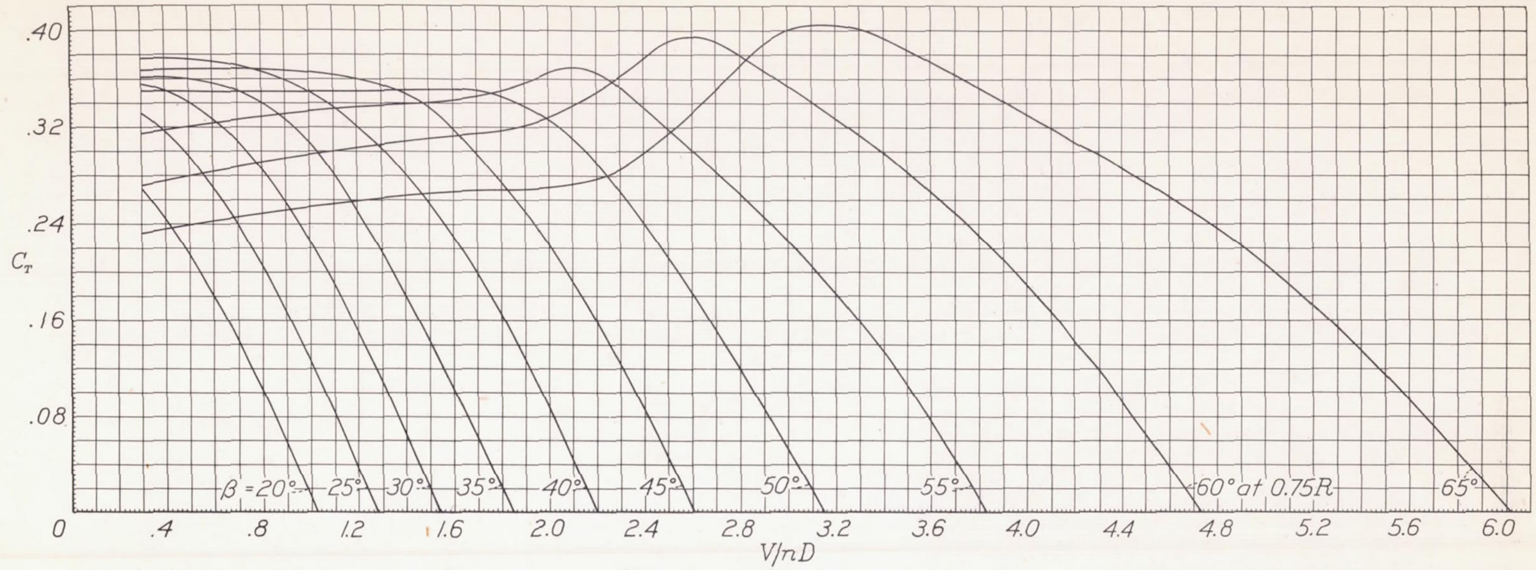

Figure 5.- Thrust-coefficient curves for 8-blade, single rotation, without wing.

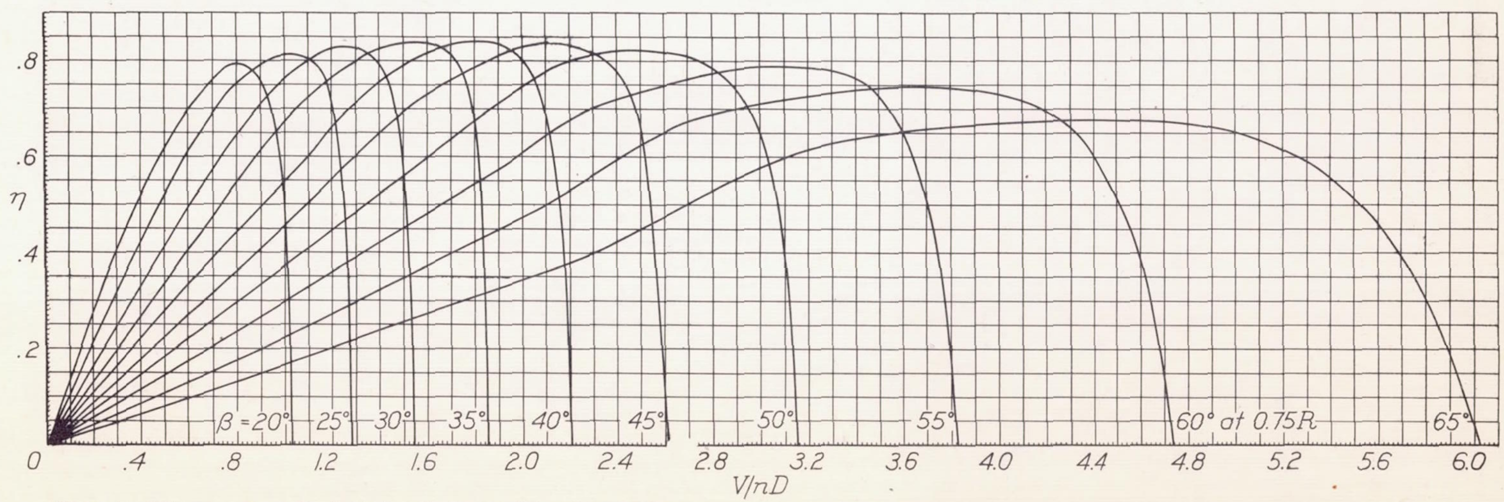

Figure 7.- Efficiency curves for 8-blade, single rotation, without wing.

NACA

Figs. 5, 7

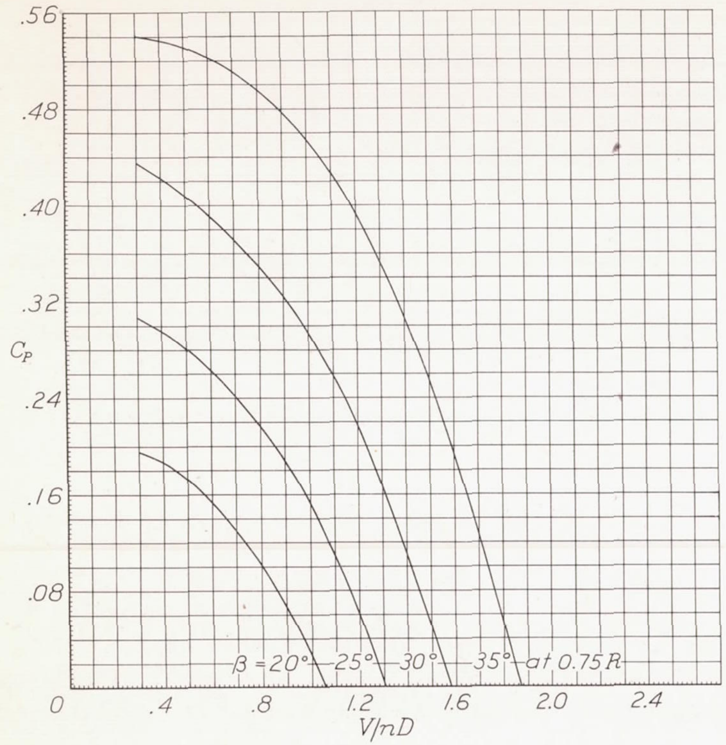

Figure 6(a).- Power-coefficient curves for 8-blade, single rotation, without wing.

Figure 13(a) - Power-coefficient curves for 8-blade single rotation with wing.

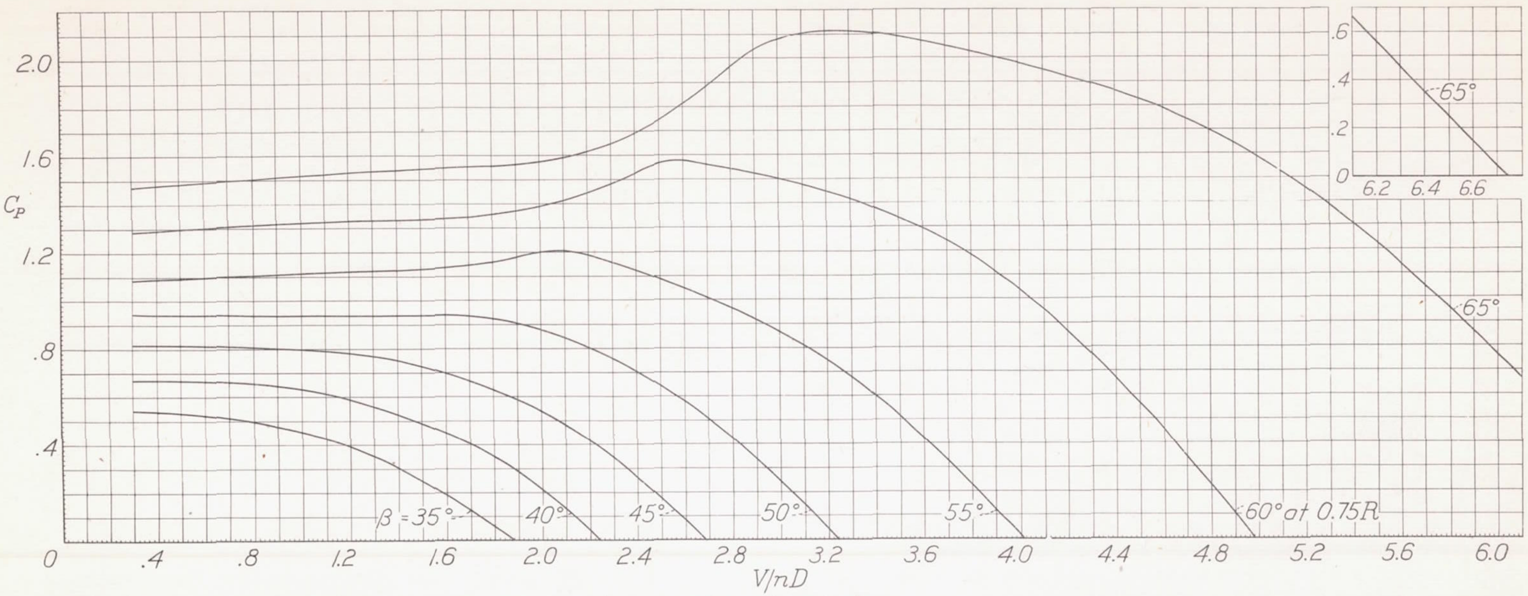

Figure 6b.- Power-coefficient curves for 8-blade, single rotation, without wing.

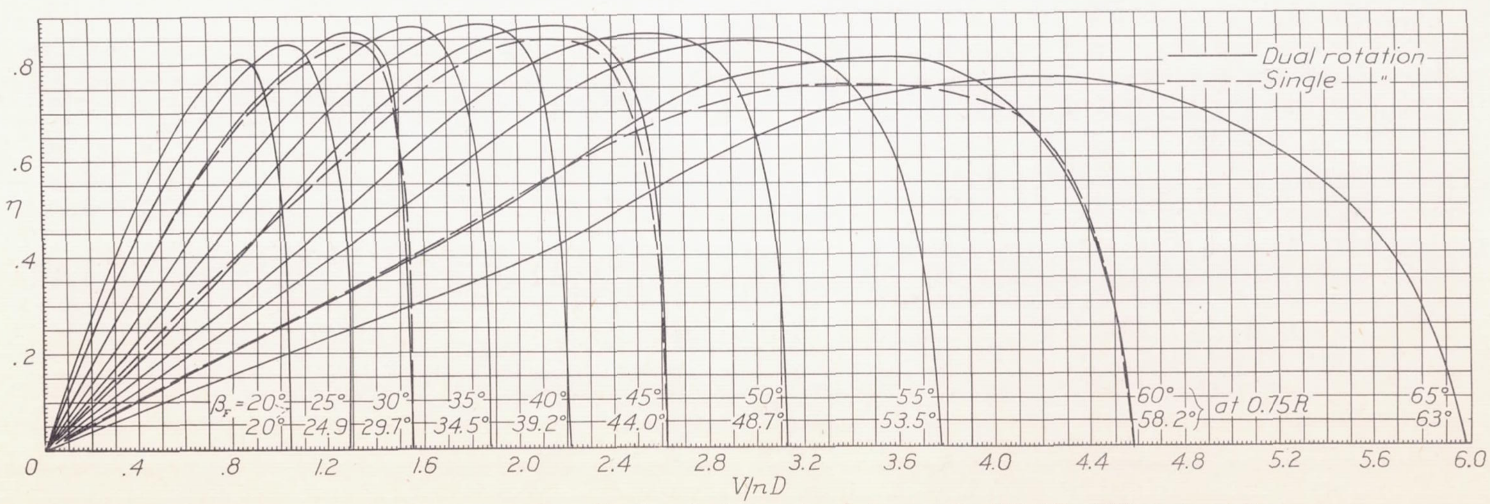

Figure 19.- Efficiency curves for 8-blade dual rotation with wing showing superimposed curves for 30°, 45° and 60° single rotation.

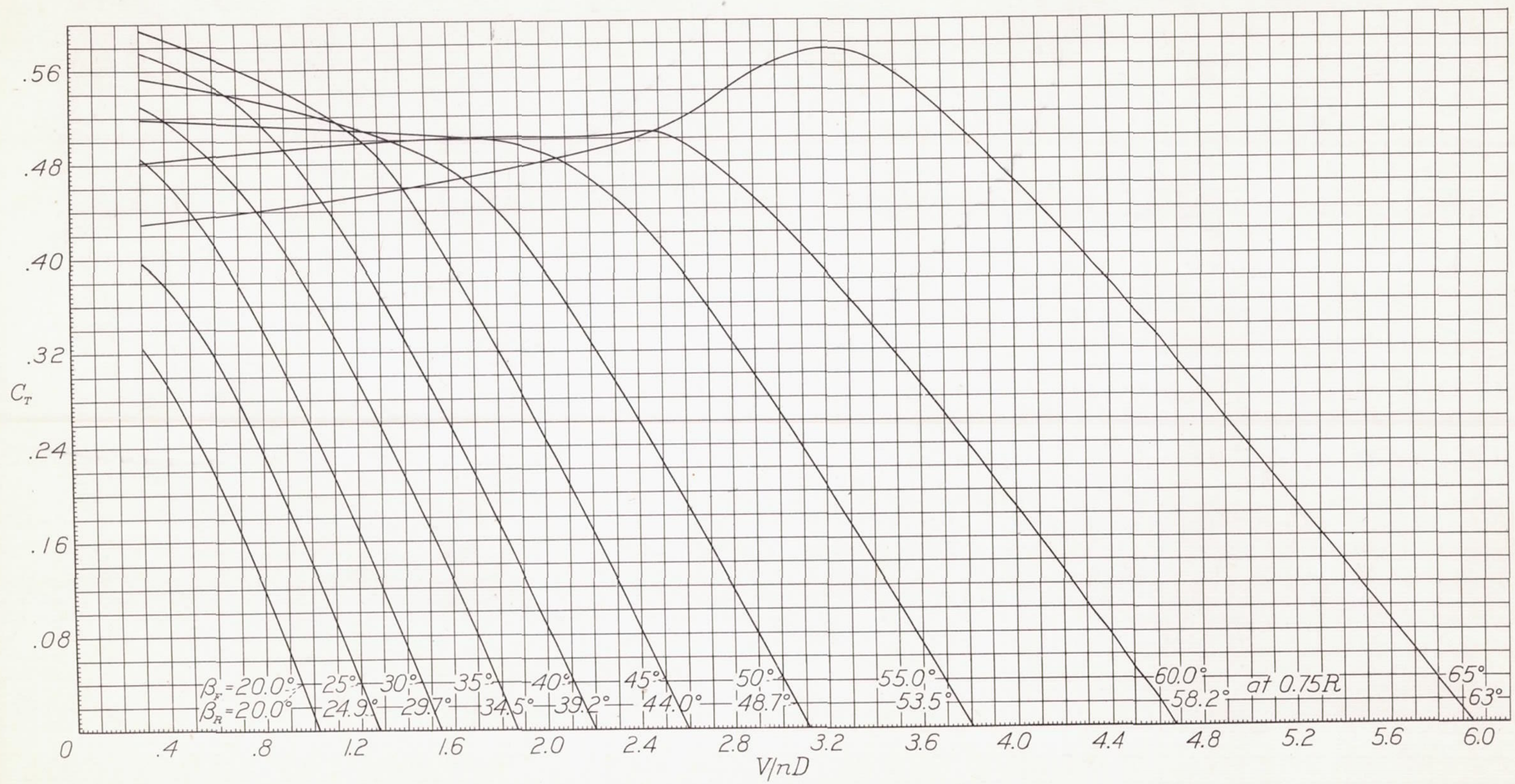

Figure 8.- Thrust-coefficient curves for 8-blade dual rotation, tractor, without wing.

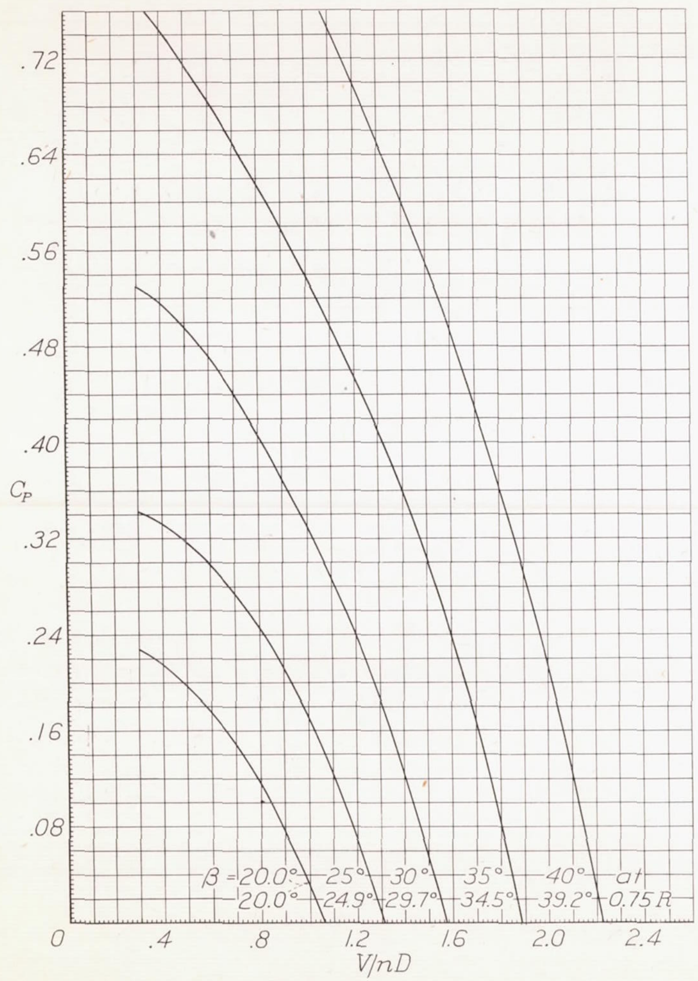

Figure 9(a).- Power coefficient curves for 8-blade,dual rotation,without wing.

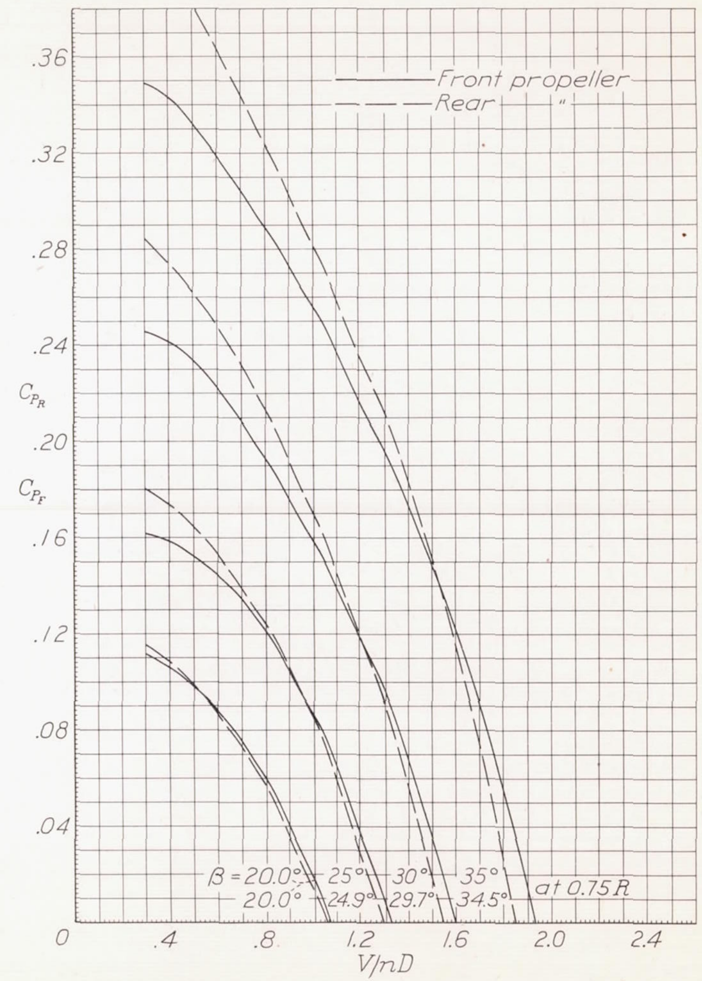

Figure 10(a).- Individual power coefficient curves for eight-blade dual rotation, tractor,without wing.

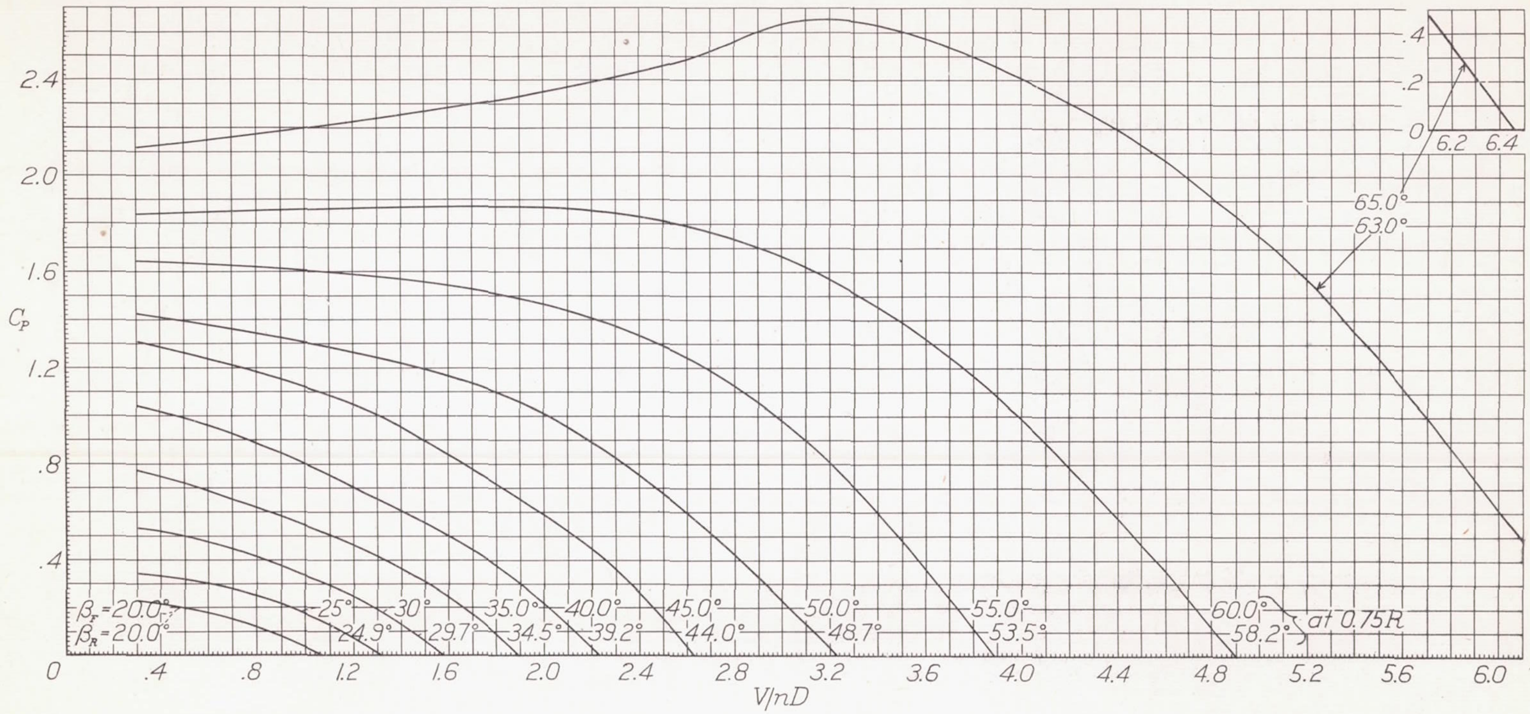

Figure 9(b).—Power-coefficient curves for 8-blade dual rotation, tractor, without wing.

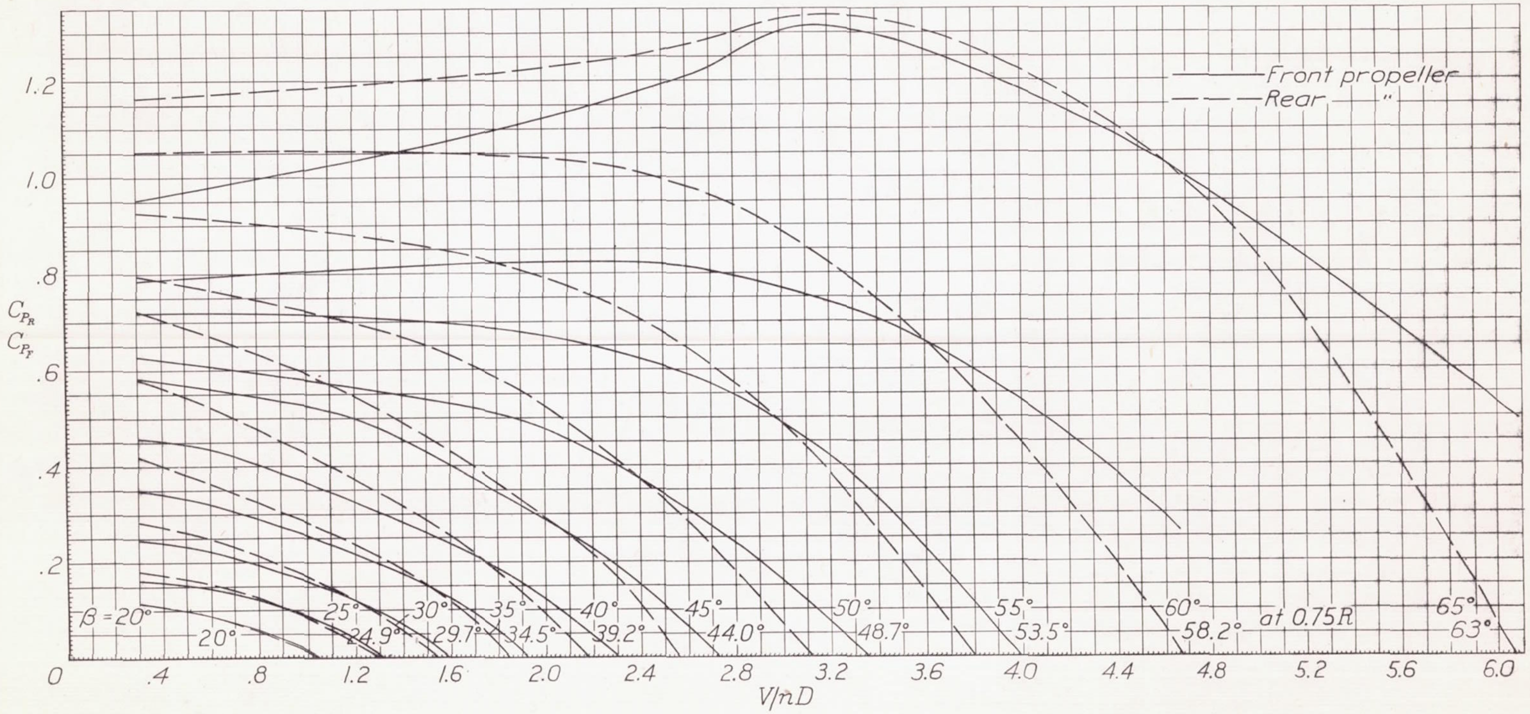

Figure 10(b).- Individual power coefficient curves for 8-blade dual rotation, tractor, without wing.

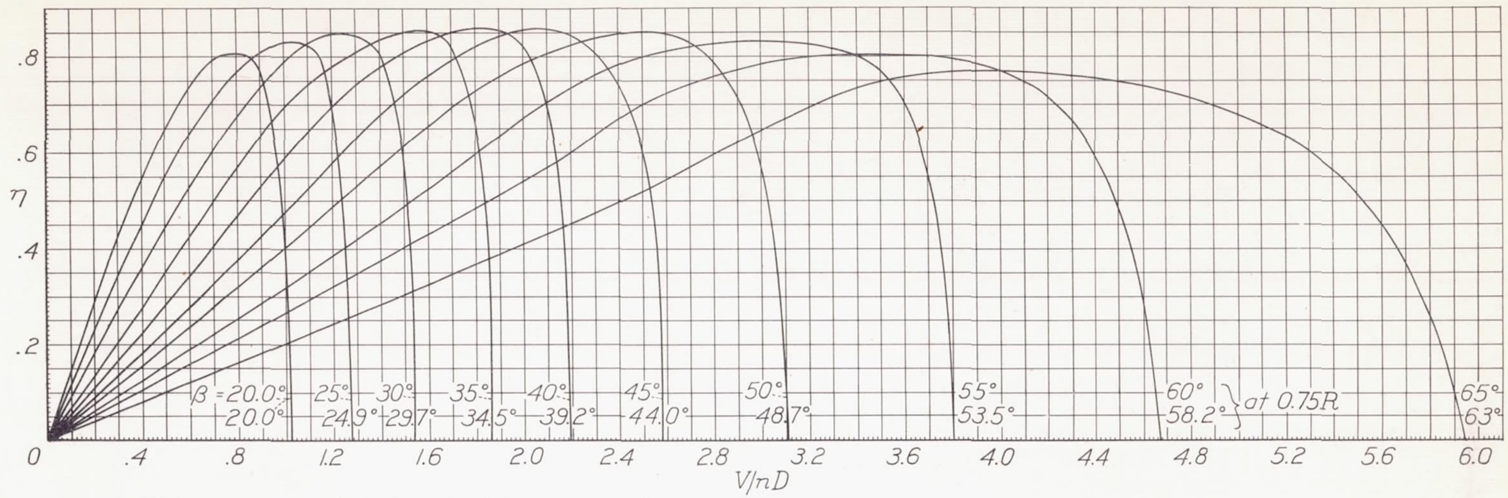

Figure 11.- Efficiency curves for 8-blade dual rotation, tractor, without wing.

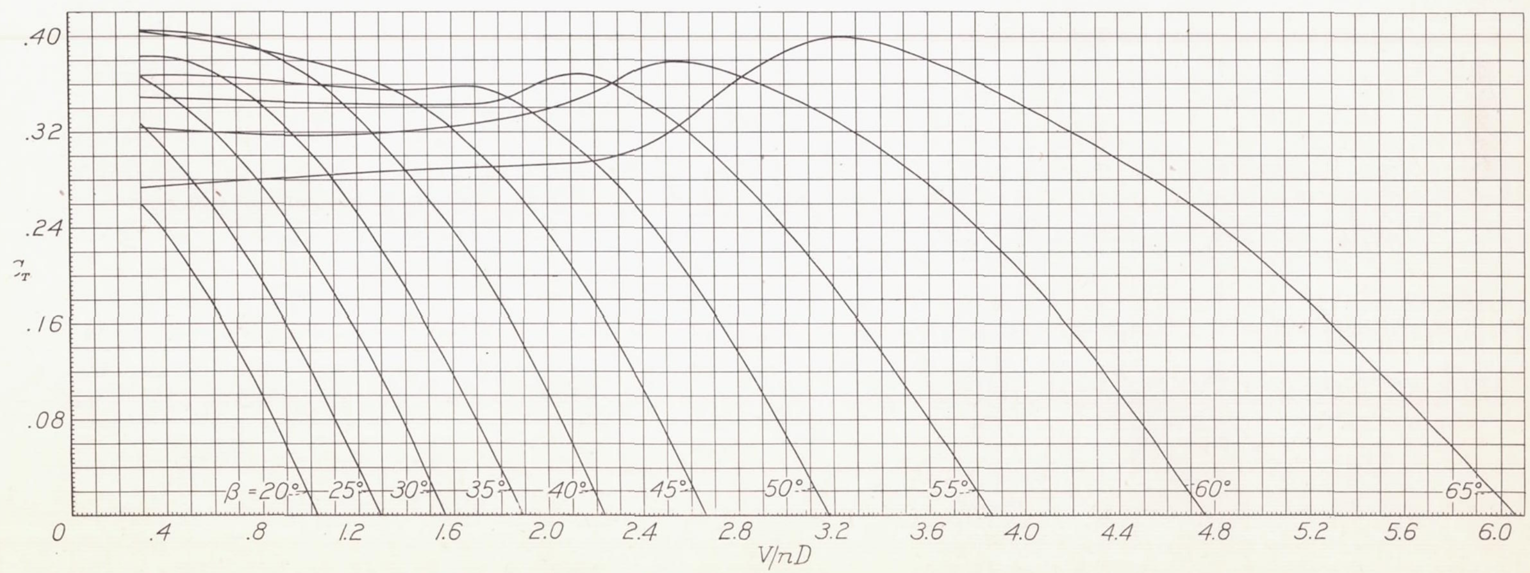

Figure 12.- Thrust-coefficient curves for 8-blade single rotation with wing.

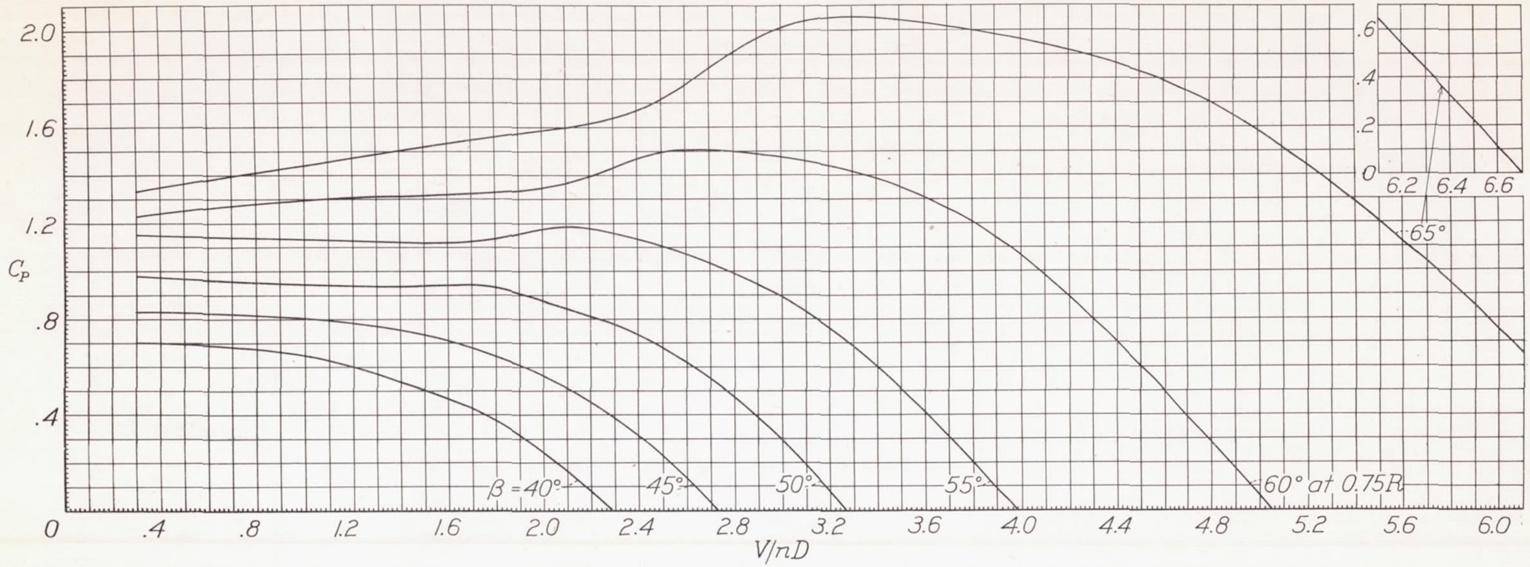

Figure 13(b).- Power-coefficient curves for 8-blade single rotation with wing.

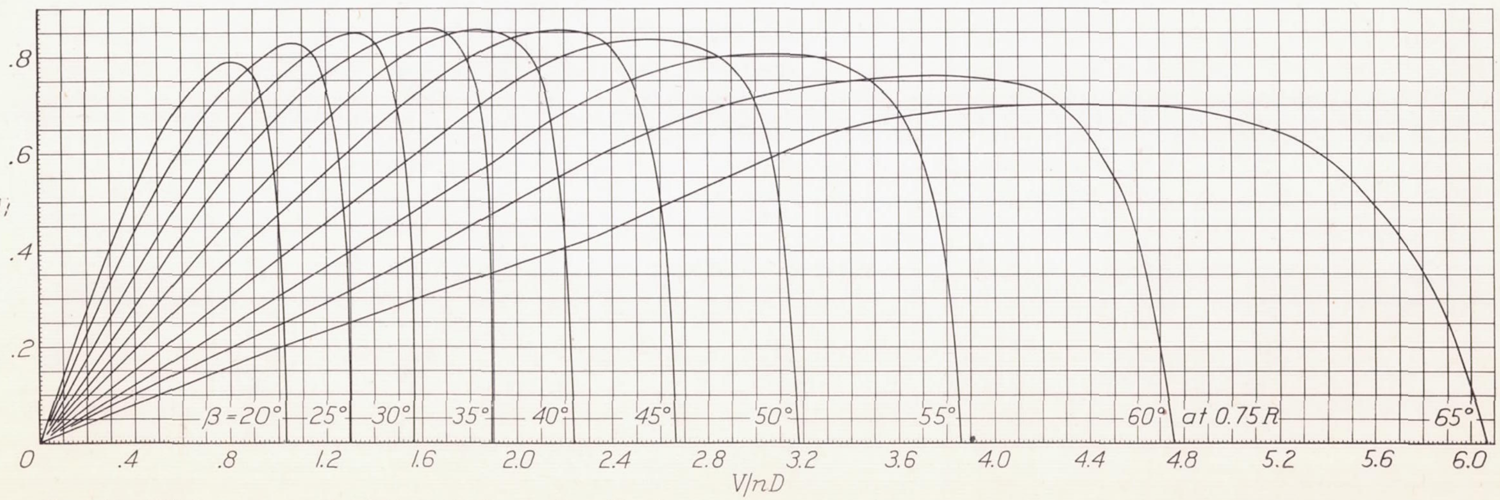

Figure 14.- Efficiency curves for 8-blade single rotation with wing.

L-384

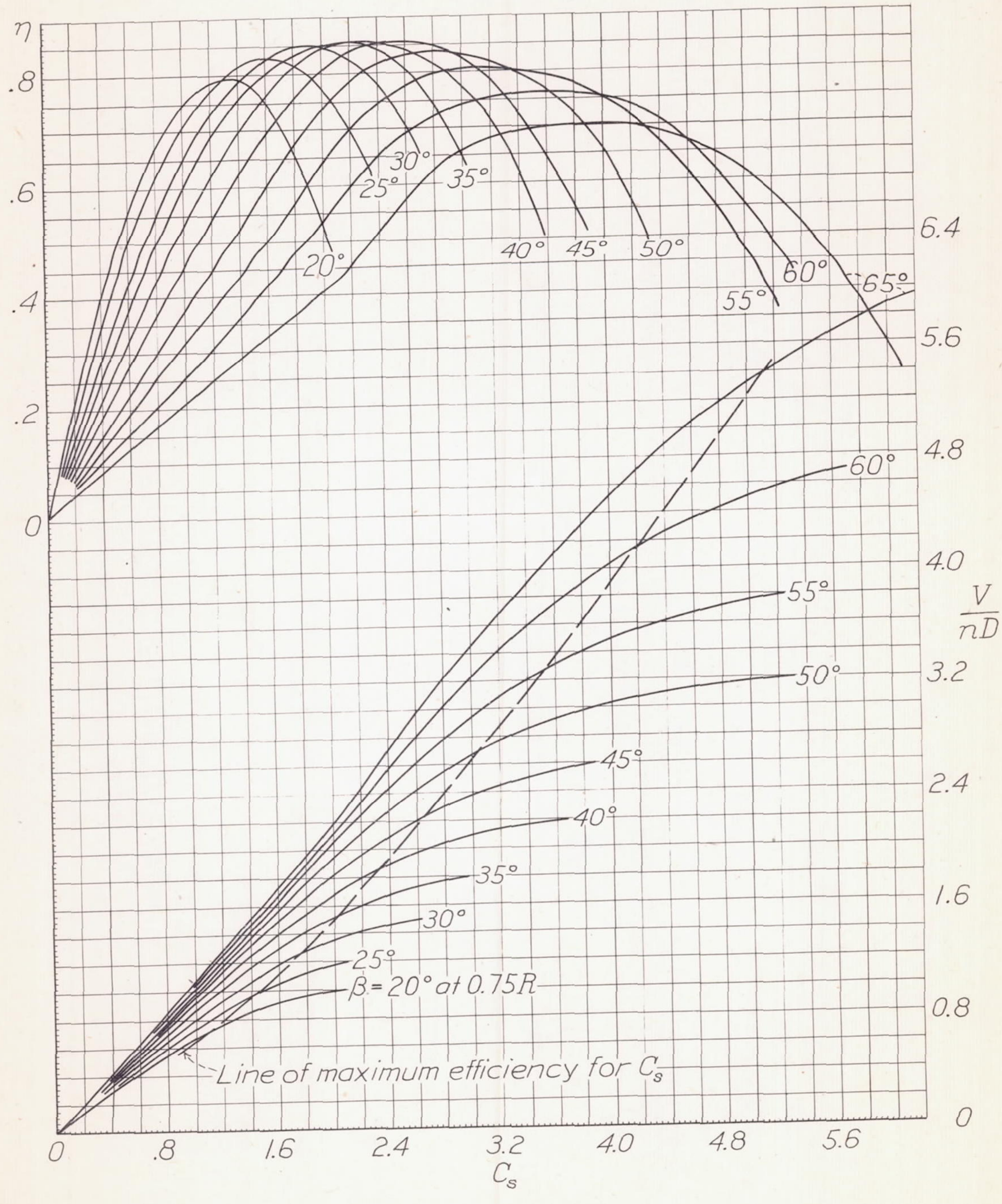

Figure 15.- Design chart for propeller 3155-6,eight-blade single rotation with wing.

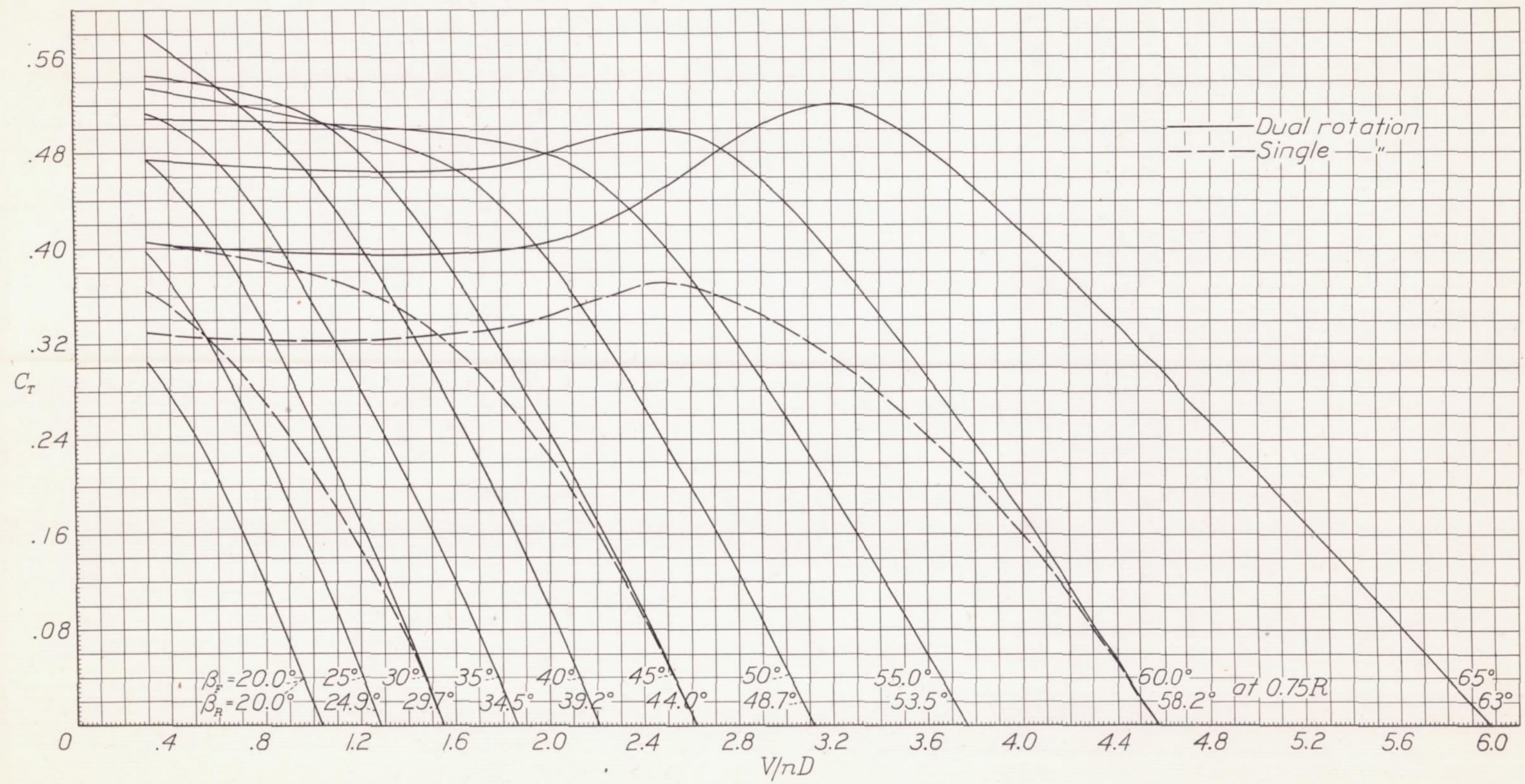

Figure 16.- Thrust coefficient curves for 8-blade dual rotation with wing, showing superimposed curves for 30° 45° and 60° single rotation.

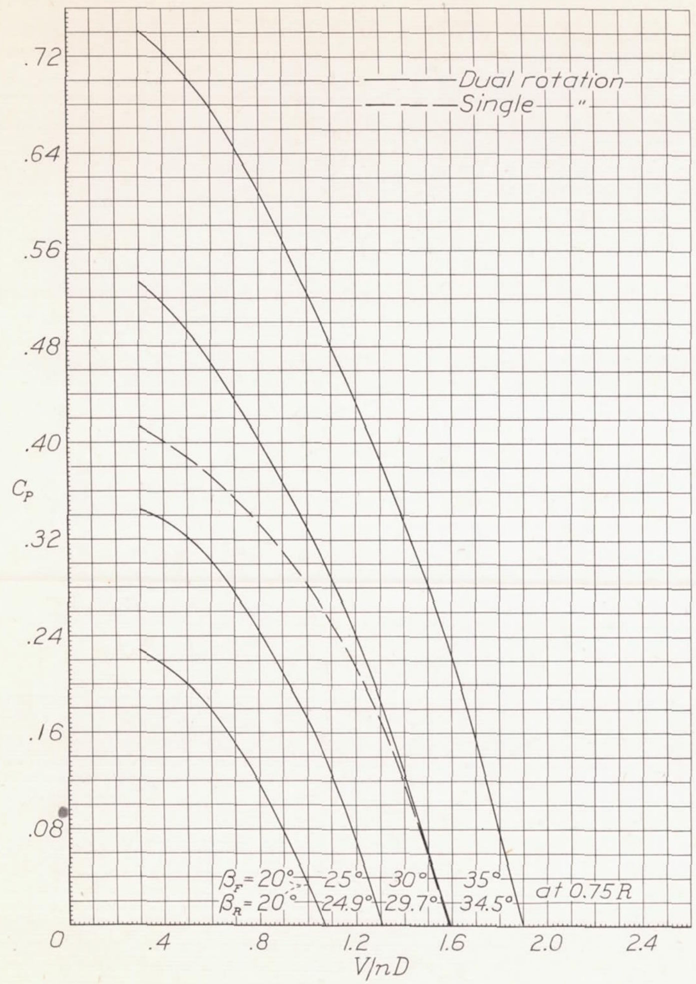

Figure 17(a).- Power coefficient curves for 8-blade dual rotation with wing, showing superimposed curve for 30° single rotation.

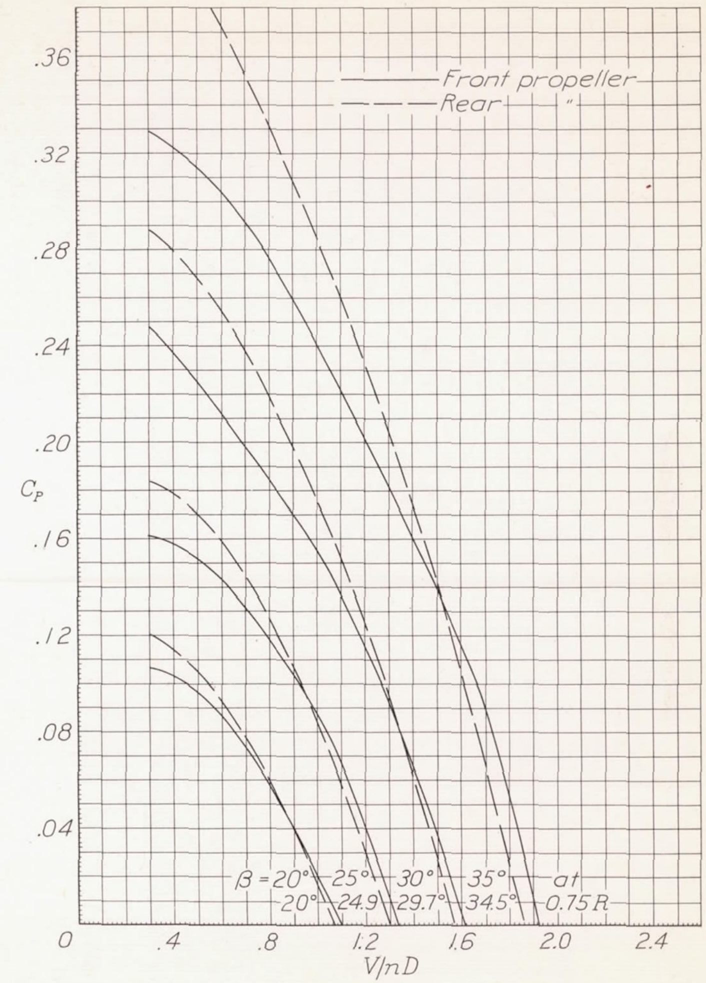

Figure 18(a).- Individual power coefficient curves for 8-blade dual rotation with wing.

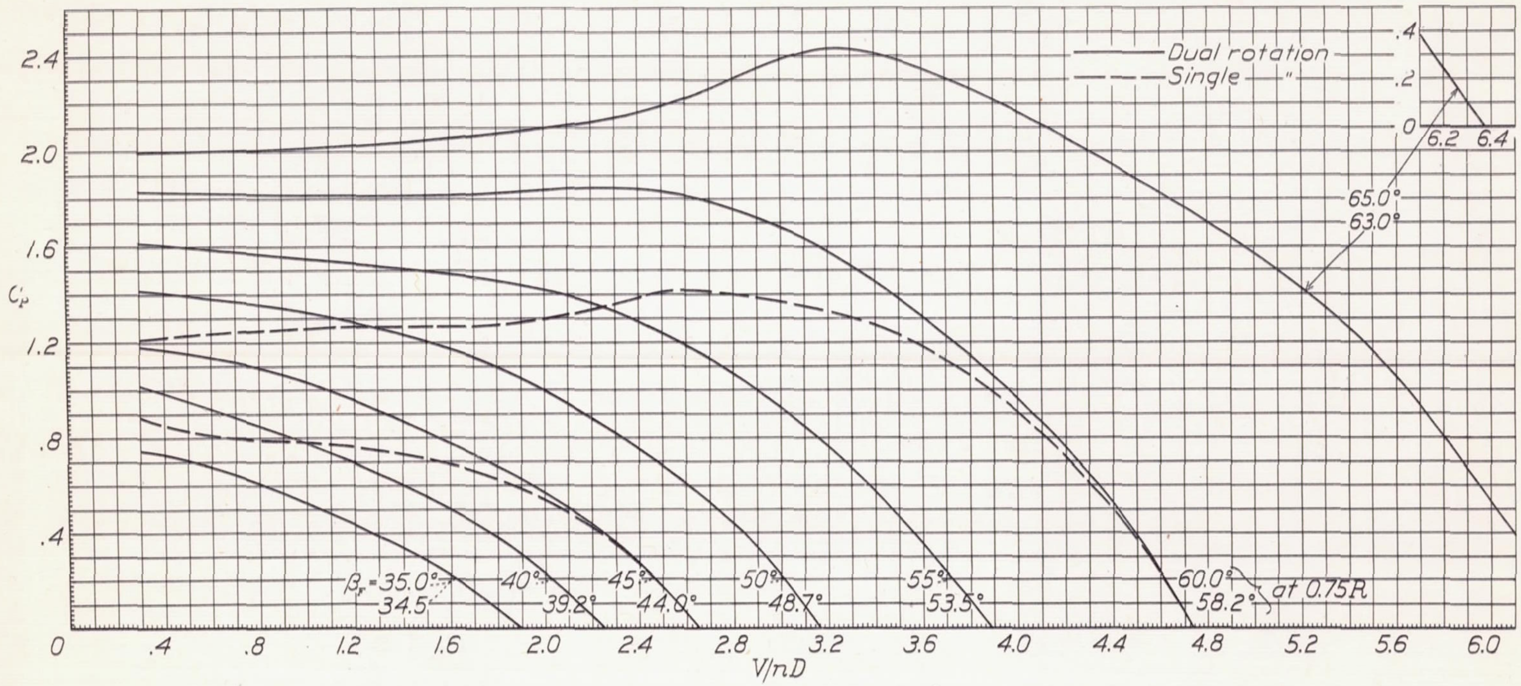

Figure 17(b).- Power coefficient curves for 8-blade dual rotation with wing, showing superimposed curves for 45° and 60° for single rotation.

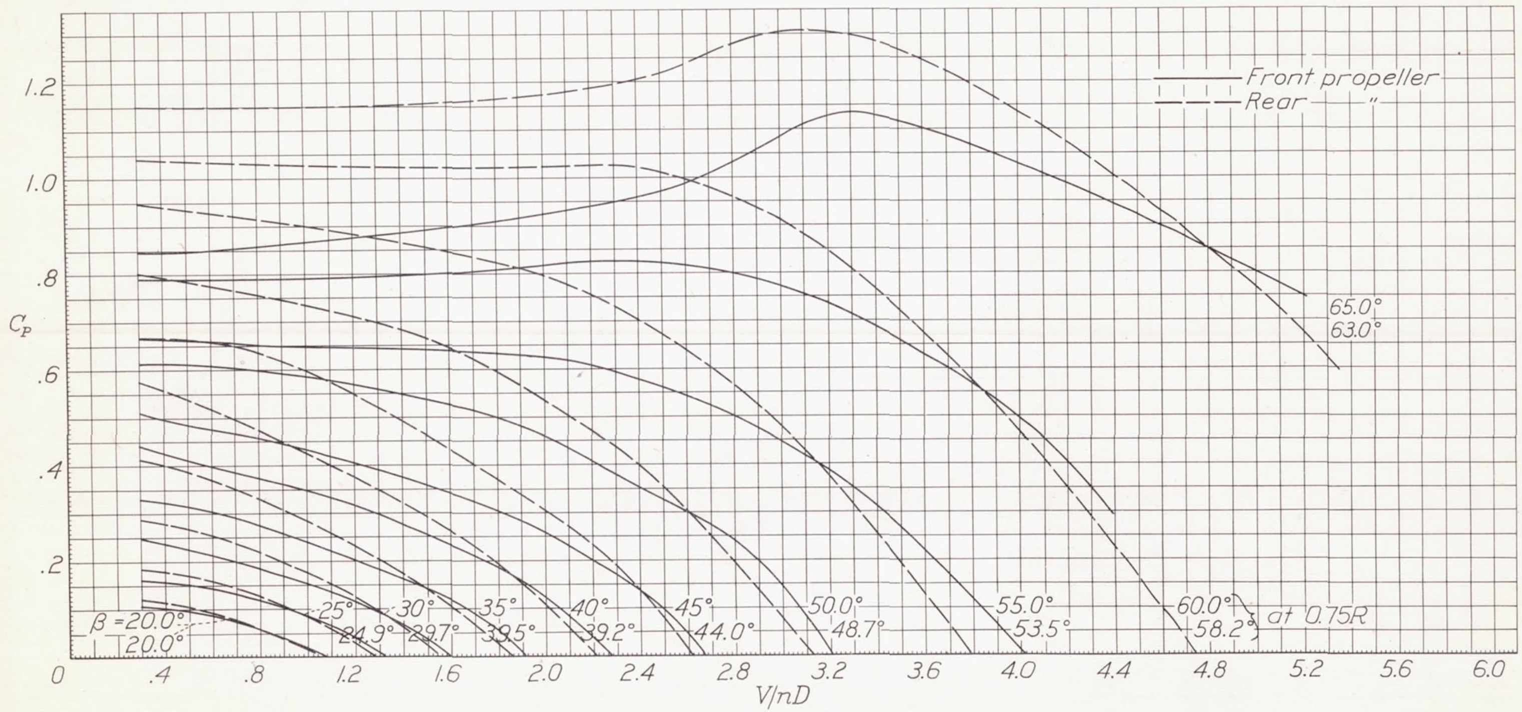

Figure 18(b).- Individual power coefficient curves for 8-blade dual rotation with wing.

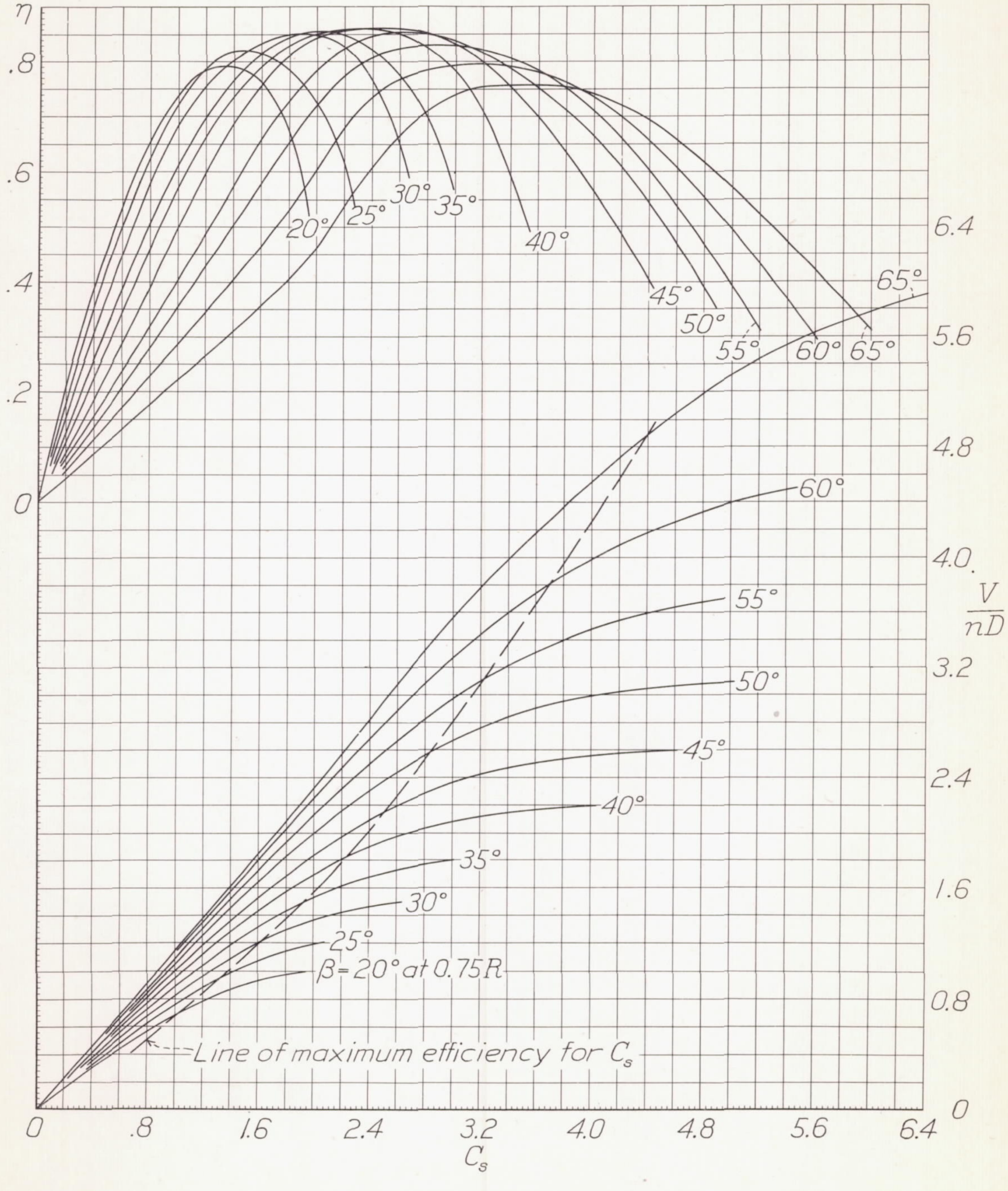

Figure 20.- Design chart for propellers 3155-6(R.H.) and 3156-6(L.H.),eight-blade dual rotation with wing.

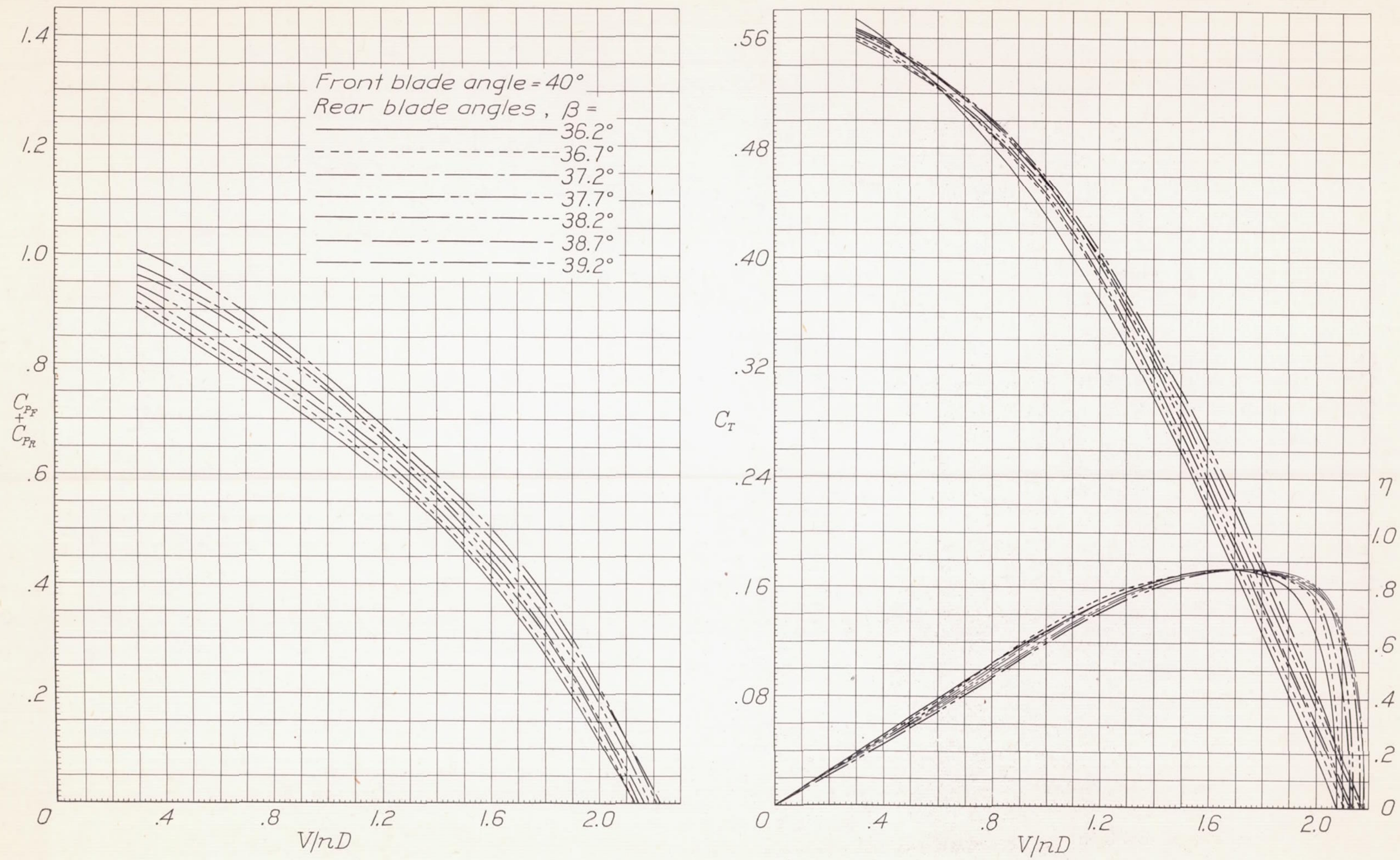

Figure 22.- Propeller curves showing the effect of small variations in rear blade angle for a front blade angle of 40°. (8-blade dual rotation propellers without wing.)

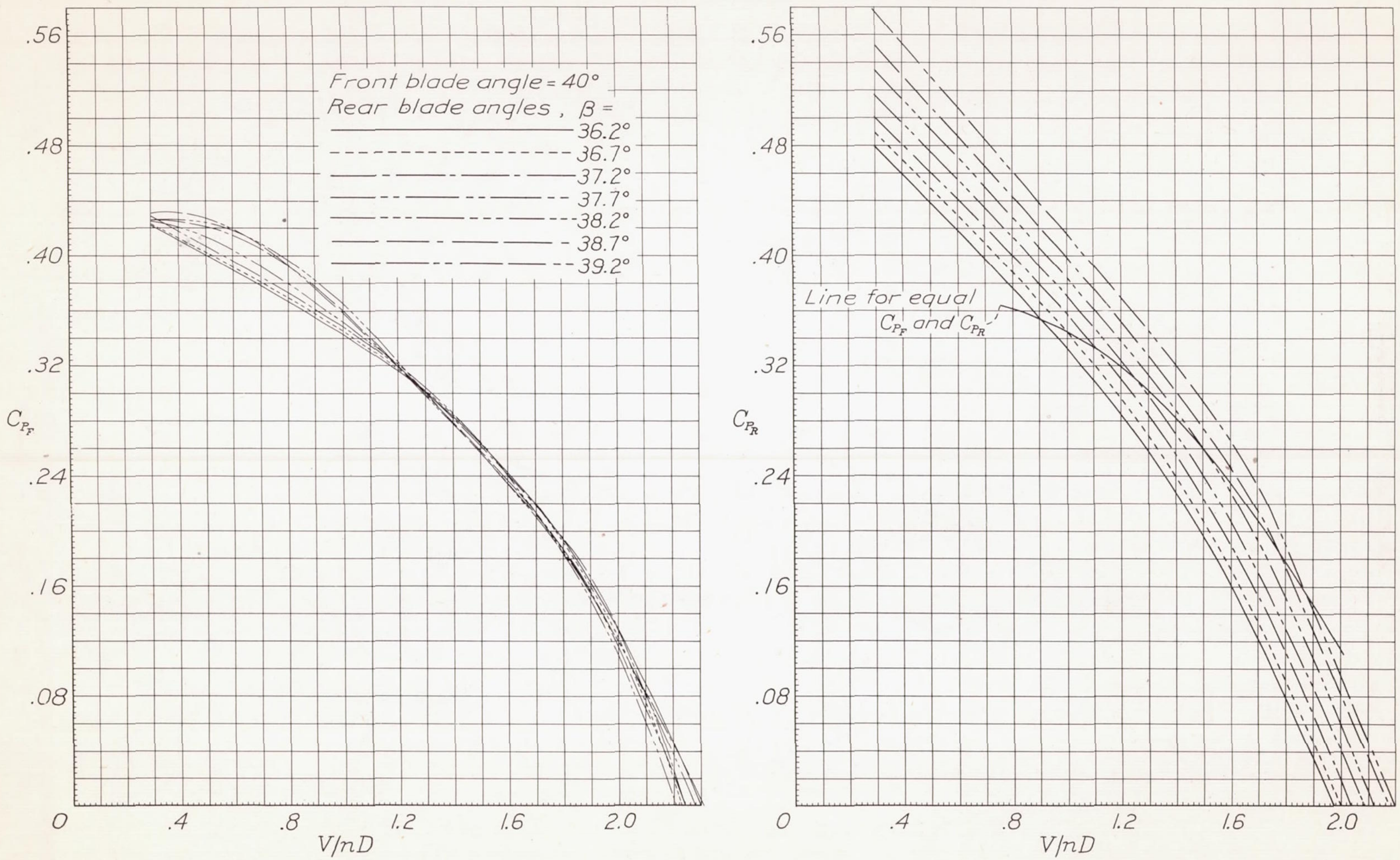

Figure 23.- Power coefficient curves showing the effect of small variations in rear blade angle for a front blade angle of 40°.
(8-blade dual rotation propellers without wing.)

L-384

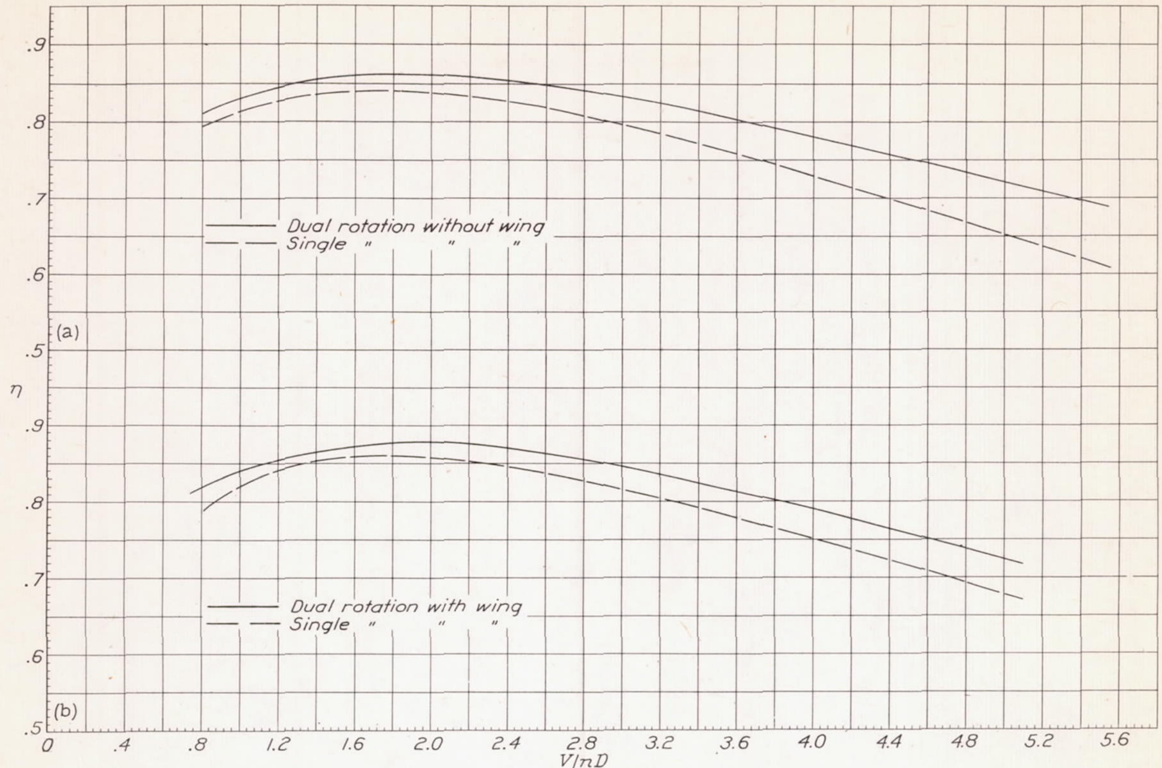

(a) Without wing (b) With wing

Figure 24.- Efficiency envelope comparisons for eight-blade propeller showing effect of dual rotation

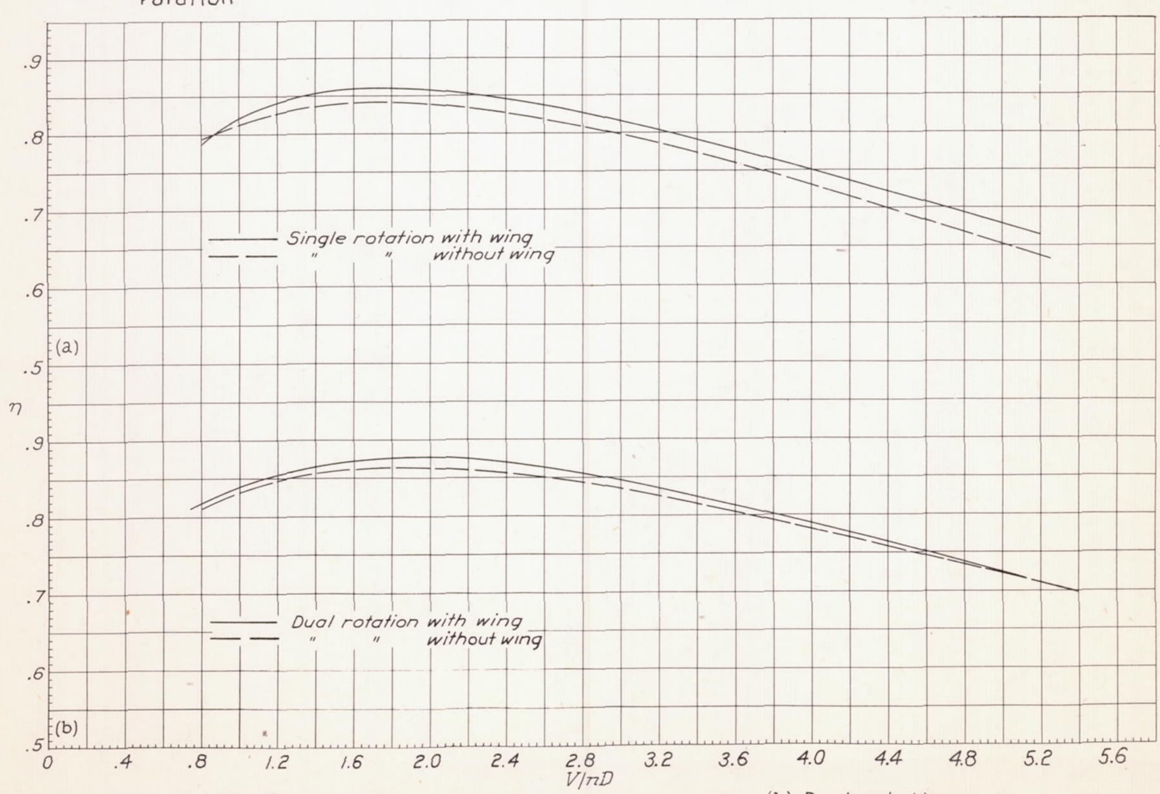

(a) Single rotation (b) Dual rotation

Figure 25.- Efficiency envelope comparisons for eight-blade propeller showing effect of wing

L-384

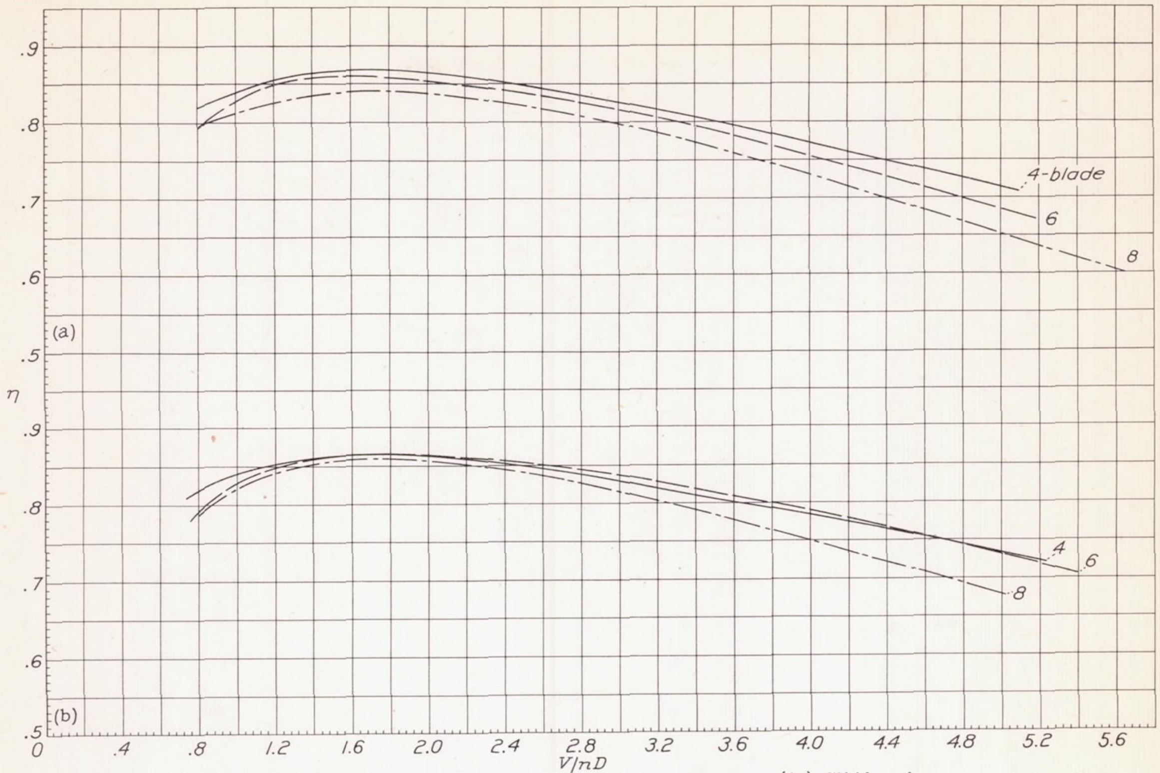

(a) Without wing. (b) With wing.

Figure 26.- Efficiency envelope comparisons for single rotation (4-and 6-blade results taken from reference 1).

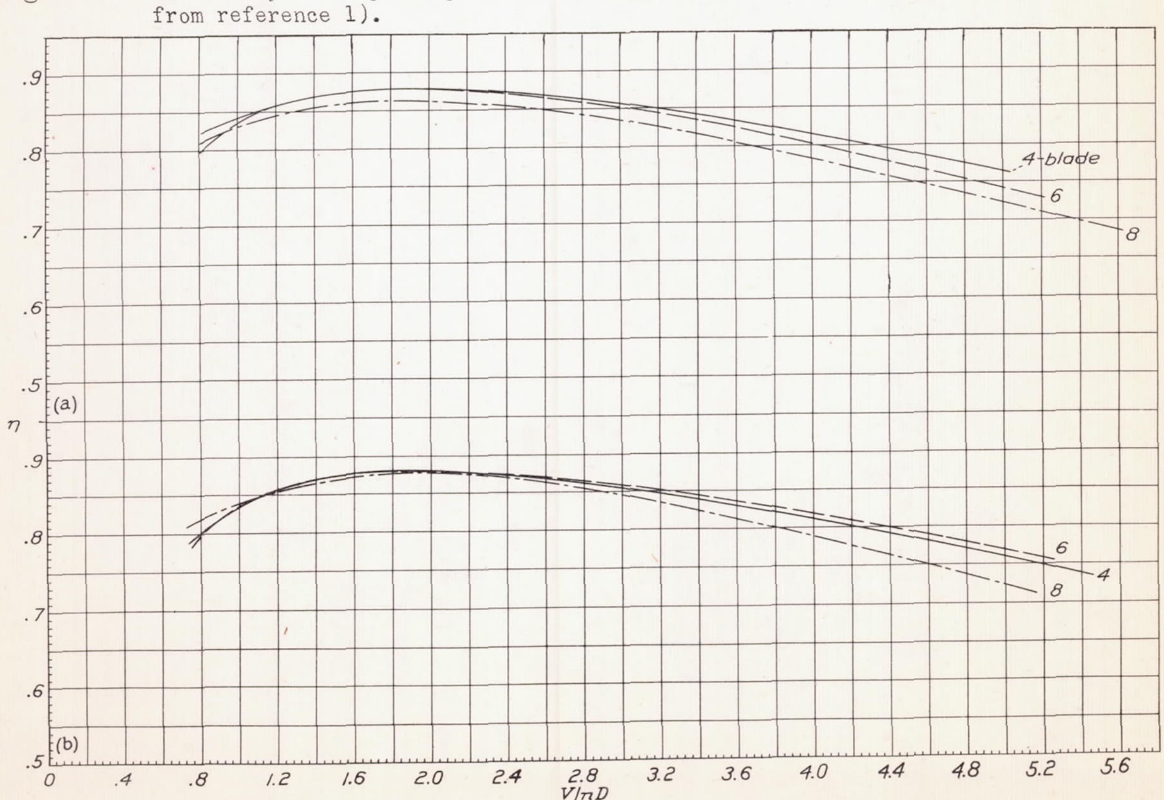

(a) Without wing. (b) With wing.

Figure 27.- Efficiency envelope comparisons for dual rotation (4-and 6-blade results taken from reference 1).

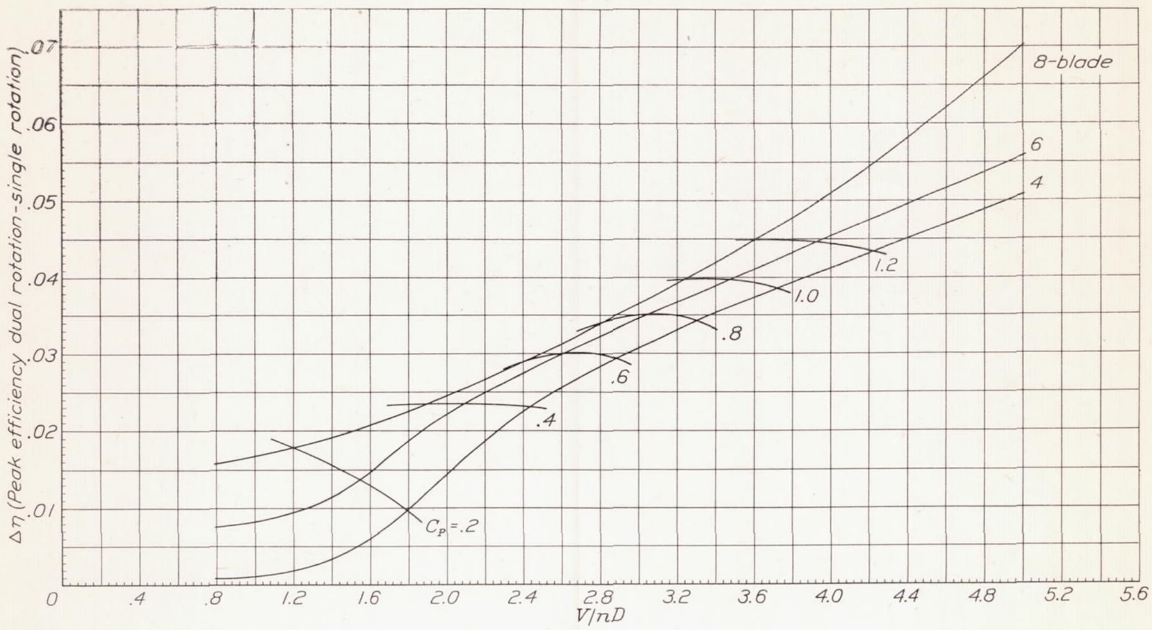

Figure 28.- Increments of peak efficiency resulting from dual rotation. Without wing (4-and 6-blade results taken from reference 1).

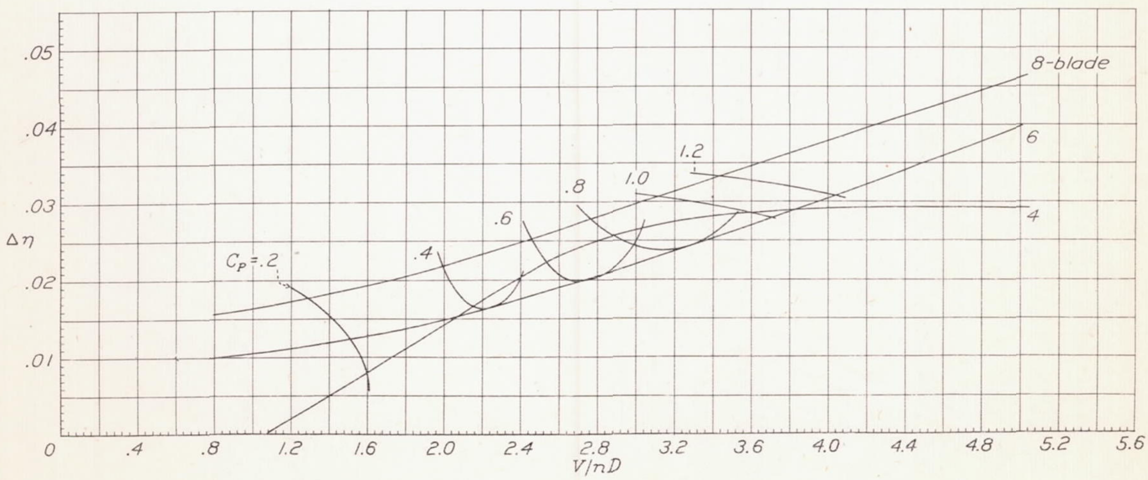

Figure 29.- Increments of peak efficiency resulting from dual rotation. With wing (4-and 6-blade results taken from reference 1).

L-384

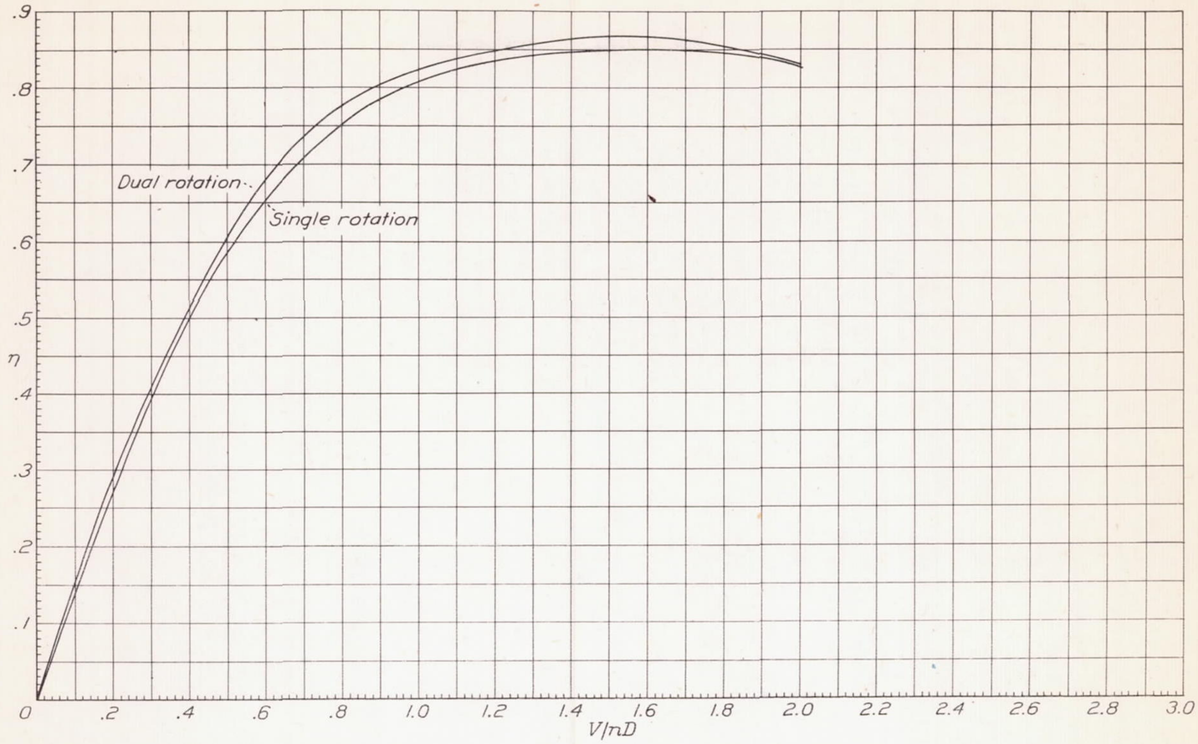

Figure 30.- Effect of dual rotation on efficiency for constant power. C_P = 0.2. With wing.

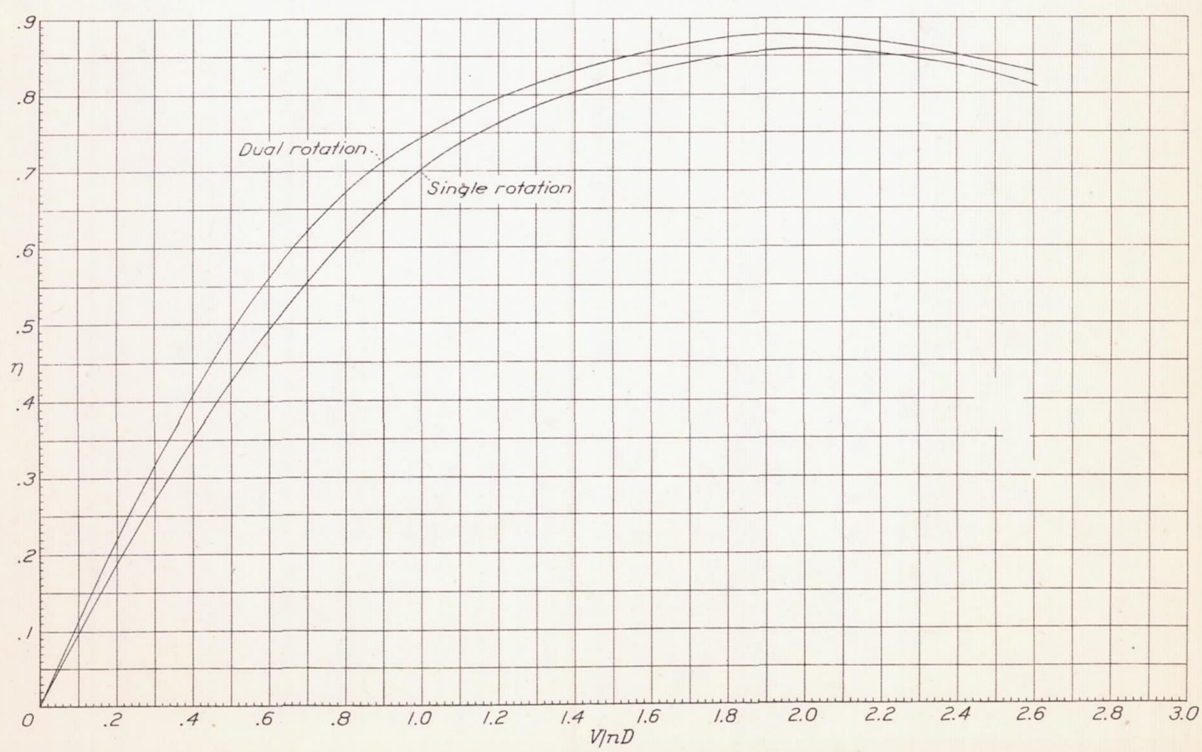

Figure 31.- Effect of dual rotation on efficiency for constant power. C_P = 0.4. With wing.

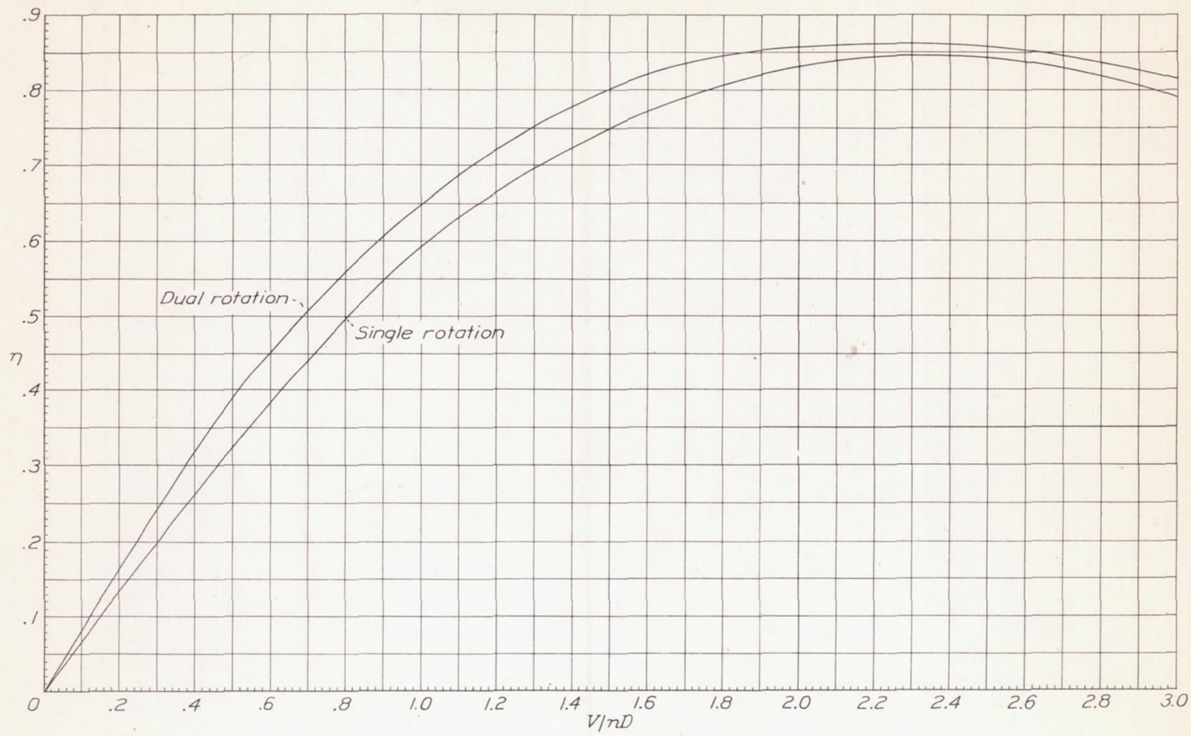

Figure 32.- Effect of dual rotation on efficiency for constant power. Cp = 0.6. With wing.

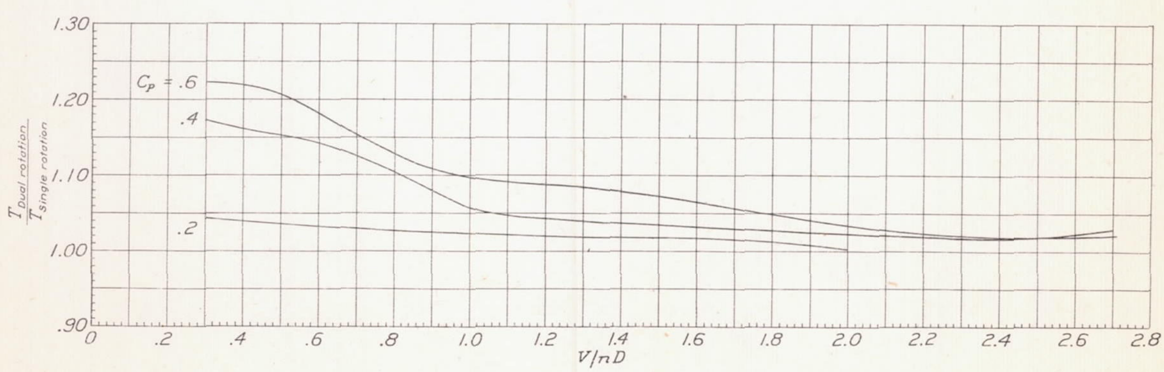

Figure 33.- Effect of dual rotation on thrust at constant power. With wing.